CONFERENCES AND SYMPOSIA

PACS numbers: 01.10.Fv, **01.60.+q**, **01.65.+g**, **02.70.–c**, 03.65.Ta, **43.30.+m**, **43.58.+z**, **89.70.–a**, 91.50.Ga **95.55.–n**, **96.30.–t**

Commemoration of the centenary of the birth of Academician V A Kotel'nikov

(Joint scientific session of the Physical Sciences Division of the Russian Academy of Sciences and the Division of Nanotechnologies and Information Technologies of the Russian Academy of Sciences, 17 September 2008)

Yu V Gulyaev, V A Kotel'nikov; L M Zelenyi, N A Armand; N A Kuznetsov, I N Sinitsyn; V I Kaevitser, V M Razmanov

DOI: 10.3367/UFNe.0179.200902f.0201

The joint scientific session of the Physical Sciences Division of the Russian Academy of Sciences and the Division of Nanotechnologies and Information Technologies of the Russian Academy of Sciences (RAS), devoted to the centenary of the birth* of Academician V A Kotel'nikov, was held on September 17, 2008 in the Rotunda Hall of RAS. The following reports were presented at the session:

(1) **Gulyaev Yu V** (Kotel'nikov Institute of Radioengineering and Electronics, RAS, Moscow) "Creative career of Vladimir Aleksandrovich Kotel'nikov (opening address)";

(2) **Pustovoit V I** (Scientific and Technical Center of Unique Instrument Making, RAS, Moscow) "Acousto-optics: modern status and prospects";

(3) **Zelenyi L M, Armand N A** (Space Research Institute, RAS, Moscow) "Vladimir Aleksandrovich Kotel'nikov and Solar System studies";

(4) **Mikaelyan A L** (Research Institute of Systems Studies, RAS, Moscow) "Research on waveguide techniques for communication systems";

(5) **Kardashev N S** (Astrocosmic Center, P N Lebedev Physical Institute, RAS, Moscow) "V A Kotel'nikov and terrestrial and space radio astronomy";

(6) **Kuznetsov N A, Sinitsyn I N** (Kotel'nikov Institute of Radioengineering and Electronics, RAS, Moscow) "Development of Kotel'nikov's sampling theorem";

(7) **Kaevitser V I, Razmanov V M** (Fryazino Branch of the Kotel'nikov Institute of Radioengineering and Electronics, RAS, Fryazino, Moscow region) "Remote sensing of sea bottom by hydroacoustic systems with complex signals";

(8) **Matyukhin V G** (Information Technologies Federal Agency, Moscow) "Information protection in an electronic State".

* Untill recently, all documents had indicated that V A Kotel'nikov was born on September 6, 1908. According to the archival document "Extract from the registration book of Varvarinskaya church in the city of Kazan' for newborn children in 1908", discovered by N V Kotel'nikova (the daughter of V A Kotel'nikov) in 2008, the day of Kotel'nikov's birth falls on August 28, 1908 (Julian calendar) or on September 10, 1908 (Gregorian calender). (*Editor's note*.)

Uspekhi Fizicheskikh Nauk **179** (2) 201 – 224 (2009)
DOI: 10.3367/UFNr.0179.200902f.0201
Translated by M V Chekhova, V I Kisin, N M Popova, and K A Postnov; edited by A Radzig

Vladimir Aleksandrovich Kotel'nikov
(06.09.1908 – 11.02.2005)

An abridge version of Yu V Gulyaev's opening address and reports 3, 6, and 7 is given below.

PACS numbers: **01.60.+q**, **01.65.+g**, **89.70.–a**
DOI: 10.3367/UFNe.0179.200902g.0201

Creative career of Vladimir Aleksandrovich Kotel'nikov (opening address)

Yu V Gulyaev

The Russian scientific community celebrated in autumn 2008 the hundredth anniversary of the birth of Academician

Vladimir Aleksandrovich Kotel'nikov — an outstanding scientist, engineer, teacher, and science administrator, one of the founders of radiophysics, informatics, radio astronomy, and cryptography in this country. His pioneering work was seminal for the burgeoning of new fields in science and technology: informatics and digital methods of signal transmission, statistical radiophysics, planetary radar, cryptography in the USSR, and large-scale studies of space.

As the journal *Uspekhi Fizicheskikh Nauk* (*Physics – Uspekhi*) has quite recently published a number of articles which discussed in detail the life and work of Vladimir Aleksandrovich Kotel'nikov [*UFN* **176** (7) 751 (2006); *Phys. Usp.* **49** 725 (2006)], I will not repeat their contents but will briefly outline the main stages of the creative life of this brilliant scientist; I will pay special attention to his last efforts which were never discussed previously on the pages of *UFN*.

This creative path in the life of Vladimir Aleksandrovich Kotel'nikov covered 78 years.

It began at the age of 19 with the creation of the first device known as 'triple characterograph' in this country. This work was carried out after V A Kotel'nikov graduated from the first year of the Moscow Higher Technical School (MVTU in *Russ. abbr.*) and was spending his summer vacations in the Nizhny Novgorod radio laboratory (1927). The paper "Triple characterograph" was published in 1928.

At the age of 24 V A Kotel'nikov was the first to give a correct mathematical formulation and prove, in the context of communications technologies, what subsequently became the classical sampling theorem (the Kotel'nikov theorem) which formed the basis of information theory, digital systems of message transmission, and the control, encoding, and processing of information [1932, Moscow Power Engineering Institute (MEI in *Russ. abbr.*)].

When he was 27 years of age, the first multichannel letter-printing radio system in the USSR was created under his leadership and with his participation; it had much better parameters than similar Western systems and was later widely used in the USSR [1935, the Research Institute of Communications of the People's Commissariat of Communications (NIIS NKS in *Russ. abbr.*)].

At 28, V A Kotel'nikov wrote two pioneering papers in which he, as one of the first to achieve it, applied probability theory to studying the efficiency of systems of signal diversity reception in a multibeam channel and proposed a general analytical method of studying nonlinear distortion of signals in various devices. Such methods were further improved and extended only at the end of the 1940s in the work of the best Soviet and foreign scientists (1936, NIIS NKS).

At the age of 30 he was awarded the degree of Candidate of Technical Sciences (an equivalent to a PhD), which was conferred on the merits of publications, without submission of a thesis (1938, Leningrad Electrotechnical Institute) and was elected Head of the Chair of Fundamentals of Radio Engineering at the Radio Engineering Department of the MEI.

At 31, V A Kotel'nikov devised unique multichannel telephone – telegraph equipment for radio communications, which for the first time used a single side frequency band; it was installed on the Moscow – Khabarovsk line (1939). At that time, this trunk line was a tremendous achievement of radio engineering in the USSR and in the world (1939, NIIS NKS).

At the age of 32 he formulated and proved the theorem of the 'one-time key' which laid the basis for the progress of cryptography and clearly defined the criteria of a mathematically nondecipherable system (1941, NIIS NKS). In the same period, he worked out a new class of nondecipherable (at the time) Soviet systems for voice encoding for classified radio communications (1941 – 1943, State Union Research Production Institute 56, city of Ufa). This equipment went through 'baptism by fire' in 1942 when wire communication lines to the Transcaucasian front were disrupted during the battle of Stalingrad. It was subsequently used to connect the Stavka Headquarters of Supreme Command to the fronts and still later for diplomatic connection lines from Moscow to Helsinki, Paris, and Vienna to conduct negotiations on signing peace treaties at the end of World War II, and also during the Tehran, Yalta, and Potsdam conferences of three Heads of States (1943 – 1945). Improved systems of this type were subsequently used with great success for governmental communications up to the 1970s.

At 36, V A Kotel'nikov revived and led the Chair of Theoretical Fundamentals of Radio Engineering at the Radio Engineering Department at the MEI, heading it for 36 years (1944 – 1980). In 1944 – 1947 he supervised the creation of telemetering instrumentation for aviation.

At 38, V A Kotel'nikov developed the theory of potential noise immunity (the topic of his DSc thesis) — one of the main branches of information theory, in which he laid the foundation of a new field of science — statistical radiophysics. This work, which was far ahead of its time, subsequently became one of the cornerstones of the modern theory of communications (1946, MEI).

At the age of 39, he became Head of the Sector of Special Tasks for research in the framework of missile and space programs (SpetsSektor in *Russ. abbr.*) (later renamed the Special Design Bureau of the MEI) — one of the leading developers of radioelectronic equipment for the space rockets programs (1947, MEI). Unique radioelectronic systems for jet engines and space vehicles for civilian and military use were developed in this framework. Many of V A Kotel'nikov's ideas are still used in creating new systems of steering and control of space apparatuses. Being the Chief Designer of the SpetsSektor in 1947 – 1953, he sat on the Interdepartmental Council of Chief Designers that was headed by S P Korolev. He was elected Dean of the MEI Radio Engineering Department (1947 – 1953).

At 45, he was elected Full Member of the USSR Academy of Sciences without even requiring the intermediate step of corresponding membership (1953) and became deputy director of the just founded Institute of Radioengineering and Electronics of the USSR Academy of Sciences (IRE RAS).

At 46, he became Director of the IRE RAS while it was being created; in a very short time it joined the group of leading research organizations in radio electronics both in this country and abroad. He headed the Institute for 33 years (1954 – 1987), and then became its Honorary Director; he continued to chair the Learned Council of the Institute for another 18 years until the end of his life. Vladimir Aleksandrovich guided the progress of many new fundamentally important areas of research and was able to complete a number of outstanding scientific and technological projects. His name is inseparable from a new field in space exploration — planetary radar.

At the age of 52, V A Kotel'nikov wrote a new page in radio astronomy: for the first time, under his supervision and with his active participation, unique experiments on the radar of Venus (1961 – 1964), Mercury (1962), Mars (1963), and

Jupiter (1963) were conducted. As a result of this work, the astronomical unit was measured with high accuracy, and a new theory of the motion of the inner planets of the Solar System was developed and confirmed by measurements. The radar survey of Venus, carried out in 1983 – 1984 by the aboard integrated radar system of automatic interplanetary probes Venus-15 and Venus-16, was an outstanding world-class achievement; it produced an image of 115 mln km^2 of the northern part of the planet with a resolution of 1 km. An analysis of the unique data allowed the creation and subsequently publication of the first *Atlas of the Venusian Surface* in the history of science (Moscow: MIIGAiK, 1989). Its editor-in-chief was Academician V A Kotel'nikov (1961 – 1989, IRE).

Along with working on scientific problems and teaching, Vladimir Aleksandrovich was doing a great deal of science administration. In 1969 – 1988, V A Kotel'nikov was acting President, Vice President, then First Vice President of the USSR Academy of Sciences (AS), and headed a number of Learned Councils of the USSR AS and then Russian Academy of Sciences, as well as some interdisciplinary scientific and technical councils and commissions; he combined all this with systematic daily work at the IRE. He was doing a great deal of work on organizing and supervising long-term exploratory and fundamental research projects at the Academy, and coordinated the research of numerous organizations in the country that specialized in various fields of modern radio engineering and electronics. By realizing his enormous scientific potential and accumulated experience, possessing his phenomenal capacity for work, and through his innate responsibility for any assignment he was given, he was able to produce results with maximum efficiency.

In 1987, Vladimir Aleksandrovich resigned from the directorship of the IRE and in 1988 from the vice-presidency of the USSR AS; still heading the learned councils and taking part in the life of the Institute, he returned to theoretical work in radiophysics.

At the age of 88 to 89, he published his last papers, which completed the circle of his work in radiophysics (1996 – 1997).

As in his younger days, he worked on these papers without assistance and published them almost on the eve of his 90th birthday. The problem he was solving was the inverse of the one he treated in his earlier publications. In those papers he determined the properties that a signal needs to have for it to be transmitted through a given channel; now he reversed it: how to select the properties of a channel in order to best transmit a given signal. As in his youth, he was again far ahead of his time. These days these results have enjoyed great popularity. Radio electronics in the past prohibited the possibility to change the channel, so one had to shape the signal. Nowadays, the channel can be selected in such a manner that it can transmit the signal in an optimal manner, and on top of that, it 'cleans' the signal too, filtering out the noise that would make it impossible to properly decode the signal at the output. These are essentially adaptive channels. These were his last scientific publications. And to top it all, he turned to quantum mechanics.

Vladimir Aleksandrovich became interested in quantum mechanics already in his youth. His creative path began (in 1927) when radio engineering was coming of age, and he just loved it, and quantum mechanics was starting to blossom and provided the major excitement for the scientific intelligentsia; these people hotly discussed the quantum mechanics papers appearing in journals. No wonder that the wave of interest in this 'mysterious' field took hold of the young Vladimir Kotel'nikov.

He started buying books on quantum mechanics that began to appear in the USSR and browsed through them — there was not enough time to do serious reading. Vladimir Aleksandrovich later remembered that each time he was left with a feeling of dissatisfaction as he felt "unable to comprehend this quantum mechanics to the very bottom." He dreamed of "some day figuring it all out."

At last he "got a bit of free time" and tackled the subject. He did not regard himself as a specialist in the field and tended to look at his new project as a "hobby for an old man."

He began by carefully reading the available books on 'classical' quantum mechanics. He decided to shun all 'alternative trends' in order to avoid undesirable influences; he wanted to see what he could produce himself. His 'square one' was the Schrödinger equation. By the end of 2003 he was ready to discuss the obtained results with specialists, but time ran out for him. V A Kotel'nikov died on February 11, 2005. The 97th year of his life ended with a nearly complete but unpublished work *Model Nonrelativistic Quantum Mechanics*; the drafts were published in 2008.

In this manuscript Vladimir Aleksandrovich presented nonrelativistic quantum mechanics (based on the Schrödinger equation) in terms of classical probability and classical concepts of the existence of trajectory of a particle and a field acting on it (see Appendix). The theory that he developed is an example of so-called theories of hidden parameters on which Luis de Broglie, D Bohm, and some others worked in the 20th century. Vladimir Aleksandrovich was unaware of the results published by these authors. He independently reproduced the entire logic of the theory of hidden parameters, introduced his own terminology and notation, and generated all the basic results of nonrelativistic quantum mechanics in his own terms. By this we mean wave packet spreading, analysis of the two-slit experiment and quantum interference, construction of the theory of stationary states, the theories of the hydrogen atom and oscillator, the theory of nonstationary states and quantum transitions, and the explanation of tunneling effect.

We who worked in the Kotel'nikov Institute of Radio-engineering and Electronics, RAS loved and respected Vladimir Aleksandrovich. We consider it our unwavering duty to sustain the creative atmosphere that he built in the Institute, and strive to follow his principles in our work.

PACS number: 03.65.Ta
DOI: 10.3367/UFNe.0179.200902h.0204

Appendix
Model Nonrelativistic Quantum Mechanics. Considerations*

V A Kotel'nikov

INTRODUCTION

Quantum mechanics considers the motion of very small bodies such as elementary particles. Experiments have

* Below, the Introduction and Chapters 1 and 2 are presented. The full text of the work was published in 2008 (Moscow: Fizmatlit, 2008), 72 pages (in Russian).

shown that this motion does not always obey the laws of classical mechanics. Quantum mechanics has turned out to be more complicated and counter-intuitive than classical mechanics. In 'classical' quantum mechanics, particles have no apparent images. They have no trajectories, cannot have definite positions and velocities simultaneously, etc. The motion of particles is determined by many rules that do not always rigorously follow from the basic laws like, for instance, in the classical mechanics of macroscopic bodies and in electrodynamics.

All this complicates learning and applying quantum mechanics, especially for those who are more inherent in figurative thinking.

In this work, a figurative model of quantum mechanics is proposed, which is in agreement with the accumulated experimental data and makes the quantum mechanics of small bodies more evident and more logically rigorous.

Chapter 1

CONSTRUCTING THE MODEL

1.1 Basic statements of nonrelativistic quantum mechanics

The basic statement of classical mechanics is as follows: the state of a particle with mass m considered as a pointlike body is determined by its position given by the radius vector $\mathbf{r}$ and its velocity $\mathbf{V}$. Knowing these parameters for a certain instant of time t and the external force that acts on the particle, we can find, using Newton's laws, all parameters of the particle motion for any instant of time.

In quantum mechanics, this turns out to be different. As experiments and their analysis have shown, the state of a particle at a given instant of time t cannot be fully described by the values of $\mathbf{r}$ and $\mathbf{V}$.

The basic statement of nonrelativistic quantum mechanics, confirmed by experiments, is as follows: if one does not take into account the spin of a particle, the state of the particle at some instant of time t is fully described by some complex function (the wavefunction) in three-dimensional space:

$$\psi(\mathbf{r}, t) = a(\mathbf{r}, t) \exp\left(\mathrm{i}\beta(\mathbf{r}, t)\right), \tag{1.1}$$

where $a(\mathbf{r}, t)$ and $\beta(\mathbf{r}, t)$ are real. The function $a(\mathbf{r}, t)$ determines the probability that the particle at some instant of time t resides at a certain point in space. For instance, the probability that at the point in time t the particle will be found within a small volume $\mathrm{d}q$ containing the end point of the radius vector $\mathbf{r}$ is given by

$$\mathrm{d}P = a^2(\mathbf{r}, t)\,\mathrm{d}q\,. \tag{1.2}$$

The function $\beta(\mathbf{r}, t)$ determines the dynamical state of the particle.

In the absence of a magnetic field, knowing $\psi(\mathbf{r}, t)$ at the initial instant of time, the mass m of the particle, and the external field forces $\mathbf{F}_{\mathrm{o}}(\mathbf{r}, t)$ acting on it, one can find $\psi(\mathbf{r}, t)$ for other points in time using the Schrödinger equation. For the nonrelativistic case, which will be the only case considered here, and in the absence of the spin and the magnetic field, it is written as follows:

$$\mathrm{i}\hbar\,\frac{\partial\psi(\mathbf{r}, t)}{\partial t} = -\frac{\hbar^2}{2m}\,\nabla^2\psi(\mathbf{r}, t) + U(\mathbf{r}, t)\,\psi(\mathbf{r}, t)\,, \tag{1.3}$$

where $\hbar = 1.05 \times 10^{-27}$ erg s is the Planck constant, and $U(\mathbf{r}, t)$ is the force function of the field acting on the particle. At the same time, the force acting on the particle equals

$$\mathbf{F}_{\mathrm{o}} = -\nabla U(\mathbf{r}, t)\,. \tag{1.4}$$

Knowing $\psi(\mathbf{r}, t)$ and m, one can, using the rules of quantum mechanics, find the other parameters of the particle's motion.

One has to use probabilistic parameters here because completely identical experiments on registering small particles never have similar outcomes. The coordinates of the particles are registered within a certain range of results, and one can only talk about the probability that the particle is found at one position or another.

The rule given above is the basic statement of nonrelativistic quantum mechanics.

1.2 Velocity of a particle in model nonrelativistic quantum mechanics

In commonly used quantum mechanics, it is claimed that a particle cannot be at a certain position and simultaneously have a certain velocity. However, quantum mechanics considers the parameters of a particle taken from the different realizations of a process with the same wavefunction.

Let us try to construct a model that would correspond to the above-given basic statement of quantum mechanics and hence to the experimental evidence but at the same time imply a certain trajectory of the particle, as is the case in macroscopic mechanics. While constructing the model, we will consider the position and the velocity of a particle for the same realization, in which position and velocity can exist simultaneously. To this end, let us first find the velocity and the acceleration of the particle if it moves according to the basic statement of quantum mechanics, i.e., it satisfies the Schrödinger equation (1.3).

Suppose that at some instant of time t the particle is at a point with radius vector $\mathbf{r}$ and has velocity $\mathbf{V}(\mathbf{r}, t)$. Let us find the probability that during a time interval $t, t + \mathrm{d}t$ the particle will cross a small area $\mathrm{d}\mathbf{S}$ (see Fig. 1).[1] During the time interval $\mathrm{d}t$, the particle moves by $\mathbf{V}\,\mathrm{d}t$. It will cross the area $\mathrm{d}\mathbf{S}$ if at some instant of time t it was at a distance of $-\lambda\mathbf{V}\,\mathrm{d}t$ $(0 < \lambda < 1)$ from one of the points of this area or, in other words, if at time t it was within a domain of volume $\mathrm{d}q = \mathbf{V}\,\mathrm{d}\mathbf{S}\,\mathrm{d}t$ adjacent to this area. According to formula (1.2), the probability of this event is $\mathrm{d}P_{\mathrm{d}S} = a^2\mathbf{V}\,\mathrm{d}\mathbf{S}\,\mathrm{d}t$.

Thus, $\mathrm{d}P_{\mathrm{d}S}$ is the probability of the particle crossing of the area $\mathrm{d}\mathbf{S}$ during the time interval $t, t + \mathrm{d}t$. For $\mathbf{V}\,\mathrm{d}\mathbf{S} < 0$, the particle will cross the area $\mathrm{d}\mathbf{S}$ in the opposite direction, and in this case $\mathrm{d}P_{\mathrm{d}S}$ will be negative.

Let us choose some volume q bounded by a closed surface S. The probability that the particle will escape from this volume, i.e., will cross the surface S, within the time interval $t, t + \mathrm{d}t$ is, according to the Ostrogradsky–Gauss theorem, given by

$$P_{-} = \mathrm{d}t \oint_S a^2\mathbf{V}\,\mathrm{d}\mathbf{S} = \mathrm{d}t \int_q \nabla(a^2\mathbf{V})\,\mathrm{d}q\,.$$

The probability that at the point in time t the particle resided within the volume q is, according to formula (1.2),

[1] Unfortunately, figures are absent both in the manuscript and the published work (Moscow: Fizmatlit, 2008). (*Editor's note*.)

equal to

$$P_t = \int_q a^2 \, \mathrm{d}q \, .$$

The probability that the particle will stay within volume q at time $t + \mathrm{d}t$ can be expressed as

$$P_{t+\mathrm{d}t} = \int_q \left(a + \frac{\partial a}{\partial t} \, \mathrm{d}t \right)^2 \mathrm{d}q = \int_q \left(a^2 + 2a \, \frac{\partial a}{\partial t} \, \mathrm{d}t \right) \mathrm{d}q \, .$$

Here, we omitted the term with $\mathrm{d}t^2$ as an infinitesimal of higher order of magnitude.

Evidently, the event 'the particle is within volume q at some instant of time t' will be necessarily succeeded by either the event 'the particle stays within volume q at some instant of time $t + \mathrm{d}t$' or the event 'the particle leaves domain q within the time interval $t, t + \mathrm{d}t$.' Therefore, one finds

$$P_t = P_{t+\mathrm{d}t} + P_- \, ,$$

or

$$P_{t+\mathrm{d}t} - P_t = -P_- \, .$$

From this equality it follows that

$$\int_q \frac{\partial a^2}{\partial t} \, \mathrm{d}q = -\int_q \nabla(a^2 \mathbf{V}) \, \mathrm{d}q \, ,$$

and, since this equality should be valid for any q, one has

$$\frac{\partial a^2}{\partial t} = -\nabla(a^2 \mathbf{V}) \, . \qquad (1.5)$$

Now, let us find the value of $\partial a^2/\partial t$ according to Schrödinger equation (1.3). We substitute $\psi(\mathbf{r}, t)$ from formula (1.1) into Eqn (1.3). Then we arrive at

$$\mathrm{i}\hbar\left(\frac{\partial a}{\partial t} + \mathrm{i}a \, \frac{\partial \beta}{\partial t}\right) \exp(\mathrm{i}\beta) = -\frac{\hbar^2}{2m} \big[\nabla^2 a + 2\mathrm{i}\nabla a \nabla \beta$$
$$+ \mathrm{i}a\nabla^2 \beta - \alpha(\nabla\beta)^2\big] \exp(\mathrm{i}\beta) + Ua \exp(\mathrm{i}\beta) \, . \qquad (1.6\mathrm{a})$$

Cancelling both sides of the above equation by $\hbar \exp(\mathrm{i}\beta)$ and setting the imaginary parts equal, we find that

$$\frac{\partial a}{\partial t} = -\frac{\hbar}{2m} \left[2\nabla a \nabla \beta + a \nabla^2 \beta\right] .$$

Further, multiplying both sides by $2a$, after some algebraic transformations we obtain

$$2a \, \frac{\partial a}{\partial t} = \frac{\partial a^2}{\partial t} = -\frac{\hbar}{2m} \left[4a\nabla a \nabla\beta + 2a^2 \nabla^2 \beta\right] , \qquad (1.6\mathrm{b})$$

or

$$\frac{\partial a^2}{\partial t} = -\frac{\hbar}{m} \, \nabla(a^2 \nabla\beta) \, . \qquad (1.6)$$

Setting equal the real parts in Eqn (1.6a) and cancelling by $a \exp(\mathrm{i}\beta)$, we find

$$-\hbar \, \frac{\partial \beta}{\partial t} = \frac{\hbar^2}{2m} \left[-\frac{\nabla^2 a}{a} + (\nabla\beta)^2\right] + U \, . \qquad (1.7)$$

We see that equations (1.5) and (1.6) will coincide if we assume

$$\mathbf{V}(\mathbf{r}, t) = \frac{\hbar}{m} \, \nabla\beta(\mathbf{r}, t) \, . \qquad (1.8)$$

Hence, *if at some instant of time t a particle is at a point with radius vector* $\mathbf{r}$, *its velocity should correspond to equation* (1.8) *in order that the Schrödinger equation and relation* (1.2) *should be satisfied.*

1.3 Forces in model nonrelativistic quantum mechanics

Let us now find the forces that should act on the particle to provide these velocities. For this, let us find the acceleration of the particle from the velocities we obtained. If a particle moves along a certain trajectory, so that one should take into account the variation of $V(\mathbf{r}, t)$ due to both $\mathbf{r}$ and t, its acceleration and velocity are known to be related by the equation (see Appendix 1)

$$\frac{\mathrm{d}\mathbf{V}}{\mathrm{d}t} = \frac{1}{2} \, \nabla(\mathbf{V}^2) - \mathbf{V} \times (\nabla \times \mathbf{V}) + \frac{\partial \mathbf{V}}{\partial t} \, . \qquad (1.9)$$

According to Eqn (1.8), the particle velocity $\mathbf{V}$ is a gradient; therefore, the vector product $\nabla \times \mathbf{V} = 0$ and, hence, one has

$$\frac{\mathrm{d}\mathbf{V}}{\mathrm{d}t} = \frac{1}{2} \, \nabla(\mathbf{V}^2) + \frac{\partial \mathbf{V}}{\partial t} \, . \qquad (1.10)$$

Note that there is a difference between $\mathrm{d}\mathbf{V}/\mathrm{d}t$ and $\partial\mathbf{V}/\partial t$. The derivative $\mathrm{d}\mathbf{V}/\mathrm{d}t$ defines the acceleration of the particle corresponding to its motion along the trajectory, while $\partial\mathbf{V}/\partial t$ is the partial derivative of $\mathbf{V}(\mathbf{r}, t)$ with respect to time, with $\mathbf{r}$ considered constant.

If we assume that the particle motion satisfies Newton's law, then the existence of acceleration requires a force acting on the particle:

$$\mathbf{F} = m \, \frac{\mathrm{d}\mathbf{V}}{\mathrm{d}t} = \frac{m}{2} \, (\mathbf{V}^2) + m \, \frac{\partial \mathbf{V}}{\partial t} \, , \qquad (1.11)$$

or, taking into account formula (1.8), we obtain

$$\mathbf{F} = \frac{m}{2} \, \nabla\left(\frac{\hbar^2}{m^2} (\nabla\beta)^2\right) + m \, \frac{\hbar}{m} \, \frac{\partial \nabla\beta}{\partial t} = \frac{\hbar^2}{2m} \, \nabla(\nabla\beta)^2 + \hbar \, \frac{\partial}{\partial t} \, \nabla\beta \, . \qquad (1.12)$$

The expression on the right-hand side of Eqn (1.12) can also be obtained from relation (1.7). Indeed, calculating the gradients of the left-hand and right-hand parts of equality (1.7), we arrive at

$$-\hbar \, \frac{\partial \nabla\beta}{\partial t} = \frac{\hbar^2}{2m} \left[-\nabla \, \frac{\nabla^2 a}{a} + \nabla(\nabla\beta)^2\right] + \nabla U \, ,$$

or

$$\frac{\hbar^2}{2m} \, \nabla(\nabla\beta)^2 + \hbar \, \frac{\partial}{\partial t} \, \nabla\beta = \frac{\hbar^2}{2m} \, \nabla \, \frac{\nabla^2 a}{a} - \nabla U \, .$$

Taking this into account, we can rewrite expression (1.12) as

$$\mathbf{F} = \frac{\hbar^2}{2m} \, \nabla \, \frac{\nabla^2 a}{a} - \nabla U = \mathbf{F}_\mathrm{q} + \mathbf{F}_\mathrm{o} = m \, \frac{\mathrm{d}\mathbf{V}}{\mathrm{d}t} \, . \qquad (1.13)$$

Here,

$$\mathbf{F}_{\mathrm{o}} = -\nabla U\,, \tag{1.14}$$

according to condition (1.4), is the external field force acting on the particle, and

$$\mathbf{F}_{\mathrm{q}} = \frac{\hbar^2}{2m}\,\nabla\,\frac{\nabla^2 a}{a} \tag{1.15}$$

is an additional force that should act on the particle to provide its motion according to the Schrödinger equation and hence there is an agreement with the experimental results. This force is determined by the modulus of the wavefunction $a(\mathbf{r}, t)$.

1.4 Model of a small particle in model nonrelativistic quantum mechanics

Based on the above considerations, the following model of a small particle is proposed. The model involves two components: a bulk one, the scalar field $a^2(\mathbf{r}, t)$ equal to the modulus of the wavefunction (1.1), and a pointlike one, being the particle moving in this field. The model field will be called the quasifield, the pointlike particle will be called the T-particle, and the combination of the quasifield and the T-particle will be called the quanton.

The dynamics of the quasifield are determined by Schrödinger equation (1.3). The motion of the T-particle obeys Newton's law (1.13), i.e., the T-particle moves as a pointlike particle in classical mechanics under the action of two forces: the classical one, F_{o} (1.14), and the quantum one, F_{q} (1.15). The existence of force F_{q} makes the difference between quantum and classical mechanics.

If the force F_{q} can be neglected in comparison with the external forces F_{o}, the motion is executed according to the rules of classical mechanics. The probability that at some instant of time t the particle will be found within a small volume $\mathrm{d}q$ containing the end of the radius vector $\mathbf{r}$ is given by expression (1.2). In this case, the velocity of the T-particle will be defined by expression (1.8). If exactly the same experiment is performed many times, each time the wavefunction, as well as the quasifield, will have the same form but the T-particle will take up different positions, with the probabilities given by Eqn (1.2). Correspondingly, for the different positions of the T-particle, its velocity will be defined by expression (1.8). Since the position of a T-particle does not enter the Schrödinger equation, the particle has no effect on its quasifield. A T-particle can sets up electromagnetic and other fields and act, through external forces, on other elementary particles.

We have considered the case where the elementary particle has a single wavefunction. This is the so-called pure case. The situation may be more complicated, with the elementary particle having one of several possible wavefunctions $\psi_1(\mathbf{r}, t), \psi_2(\mathbf{r}, t), \ldots, \psi_n(\mathbf{r}, t)$, with the probabilities $P_1, P_2, \ldots, P_n$. This is the so-called mixed case, when the situation should be considered separately for each wavefunction, and the results should be summed up with an account for the probabilities $P_1, P_2, \ldots, P_n$.

Nonrelativistic quantum mechanics can be constructed from the proposed model of an elementary particle, alluding to the fact that the model does not contradict the experiment. The rest, including the Schrödinger equation, can be logically derived from this model.

Chapter 2

QUASIFIELD

2.1 Let us consider the properties of the quasifield in more detail. According to Eqn (1.2), the probability that at some instant of time t the T-particle will be found within some domain q equals

$$P_q(t) = \int_q a^2(\mathbf{r}, t)\,\mathrm{d}q\,, \tag{2.1}$$

where integration is taken over this domain. Let us call $a^2(\mathbf{r}, t)$ the **density** of the quasifield at point $\mathbf{r}$ and some instant of time t, and the integral (2.1) the **amount** of the quasifield within volume q. Then, the following statement will be valid: the probability that a T-particle is found within some domain is equal to the amount of the quasifield in this domain.

The quasifield, which can be viewed as some gas or compressible fluid with the density $a^2(\mathbf{r}, t)$, neither appears nor disappears with time but only moves with the velocity $V(\mathbf{r}, t)$. Under these conditions, the quasifield must satisfy the relation

$$\mathrm{d}t\,\frac{\partial}{\partial t}\int_q a^2\,\mathrm{d}q = -\mathrm{d}t\oint_S a^2\mathbf{V}\,\mathrm{d}\mathbf{S}\,. \tag{2.2}$$

The left-hand integral in formula (2.2) is taken over some domain q, while the right-hand one, over the closed surface S surrounding it. During a time $\mathrm{d}t$, the amount of quasifield in domain q will be reduced by the value of the left-hand side of expression (2.2). This reduction will be only due to the field escaping through the surface S. The amount of the quasifield escaping through an element $\mathbf{dS}$ of the surface during a time $\mathrm{d}t$ will be equal to $a^2\mathbf{V}\,\mathrm{d}\mathbf{S}\,\mathrm{d}t$, while the amount escaping through the whole surface will be equal to the right-hand side of equation (2.2).

2.2 Let us now find the velocity $V(\mathbf{r}, t)$ of the quasifield required in order to satisfy both relation (2.2) and the condition that the quasifield density $a^2(\mathbf{r}, t)$ correspond to the wavefunction $\psi(\mathbf{r}, t) = a(\mathbf{r}, t)\exp\big(\mathrm{i}\beta(\mathbf{r}, t)\big)$, which is the solution to the Schrödinger equation. For this, let us utilize the theorem[2] from Appendix 2, assuming in (A2.3) that

$$\psi_1 = \psi_2 = a\exp(\mathrm{i}\beta)\,.$$

Then, taking into account that $\nabla\psi_{1,2} = (\nabla a)\exp(\mathrm{i}\beta) + \mathrm{i}(\nabla\beta)a\exp(\mathrm{i}\beta)$, we obtain

$$\begin{aligned}\frac{\partial}{\partial t}\int_q & a\exp(\mathrm{i}\beta)a\exp(-\mathrm{i}\beta)\,\mathrm{d}q \\ &= \mathrm{i}\,\frac{\hbar}{2m}\oint_S\Big\{a\exp(-\mathrm{i}\beta)\big[(\nabla a)\exp(\mathrm{i}\beta) + \mathrm{i}(\nabla\beta)a\exp(\mathrm{i}\beta)\big] \\ &\quad - a\exp(\mathrm{i}\beta)\big[(\nabla a)\exp(-\mathrm{i}\beta) - \mathrm{i}(\nabla\beta)a\exp(-\mathrm{i}\beta)\big]\Big\}\,\mathrm{d}\mathbf{S}\,.\end{aligned}$$

[2] This theorem states: "*If $\psi_1(\mathbf{r}, t)$ and $\psi_2(\mathbf{r}, t)$ vary in time according to the same Schrödinger equation, namely*

$$\mathrm{i}\hbar\,\frac{\partial}{\partial t}\,\psi_1 = -\frac{\hbar^2}{2m}\,\nabla^2\psi_1 + U\psi_1\,, \tag{A2.1}$$

$$\mathrm{i}\hbar\,\frac{\partial}{\partial t}\,\psi_2 = -\frac{\hbar^2}{2m}\,\nabla^2\psi_2 + U\psi_2\,, \tag{A2.2}$$

then

$$\frac{\partial}{\partial t}\int_q \psi_1^*\psi_2\,\mathrm{d}q = \mathrm{i}\,\frac{\hbar}{2m}\int_S\left(\psi_1^*\,\nabla\psi_2 - \psi_2\,\nabla\psi_1^*\right)\mathrm{d}\mathbf{S}\,. \tag{A2.3}$$"

(*Editor's note.*)

After simplifying this expression, we get

$$\frac{\partial}{\partial t}\int_q a^2\,\mathrm{d}q = -\frac{\hbar}{m}\oint_S (\nabla\beta)\,a^2\,\mathrm{d}\mathbf{S}\,.$$

Comparing this expression with Eqn (2.2), we see that they will coincide if the quasifield velocity is assumed to be

$$\mathbf{V}(r,t) = \frac{\hbar}{m}\,\nabla\beta(r,t)\,. \tag{2.3}$$

Thus, we can assume in the model that *the quasifield cannot disappear or appear but can only move with the velocity given by expression* (2.3).

If the integration domain is assumed to be the whole space occupied by the quasifield, where $a \neq 0$, then the integral of the right-hand side of expression (2.2) will be equal to zero, since in this case $a = 0$ on the surface S.

Thus, the full amount of the quasifield of an elementary particle is always constant. This amount will be equal to the probability that the T-particle is found somewhere in the quasifield, and this probability equals unity. Hence, it follows that *the full 'amount' of the quasifield of an elementary particle is always equal to unity, i.e., the integral* (2.1) *taken over the whole field should be equal to unity*:

$$\int_Q a^2(\mathbf{r},t)\,\mathrm{d}q = 1\,. \tag{2.4}$$

Hereafter, the subscript Q of an integral means that integration is performed over the whole space where $a^2 \neq 0$.

2.3 Comparing expressions (1.8) and (2.3) we see that *the velocity of a* T-*particle is equal to the velocity of travel of the quasifield at the point where the* T-*particle is placed, i.e., the particle is entrained by the quasifield and moves together with it*.

Since the velocities of the quasifield and the T-particle are equal, their accelerations should also be equal. Therefore, an element of the field moving along some trajectory will have acceleration, according to formula (1.13), equal to

$$\frac{\mathrm{d}\mathbf{V}}{\mathrm{d}t} = \frac{\hbar^2}{2m^2}\,\nabla\,\frac{\nabla^2 a}{a} - \frac{1}{m}\,\nabla U_0\,. \tag{2.5}$$

The second term in the right-hand side of this equation is determined by external forces, while the first term, by the forces of the field itself. It depends on the field density and its derivatives at the point where the T-particle is placed, namely, on the parameter $\nabla^2 a/a$, which will often occur further. Therefore, let us consider it in more detail.

2.4 Let the origin of the coordinate system be put at our point of interest. Let us represent a as a Taylor series and limit the domain of consideration, so that the quadratic terms are sufficient. We will get

$$a(x,y,z) = \frac{1}{2}\frac{\partial^2 a}{\partial x^2}\,x^2 + \frac{1}{2}\frac{\partial^2 a}{\partial y^2}\,y^2 + \frac{1}{2}\frac{\partial^2 a}{\partial z^2}\,z^2 + \frac{\partial^2 a}{\partial x\,\partial y}\,xy + \frac{\partial^2 a}{\partial y\,\partial z}\,yz + \frac{\partial^2 a}{\partial z\,\partial x}\,zx + \frac{\partial a}{\partial x}\,x + \frac{\partial a}{\partial y}\,y + \frac{\partial a}{\partial z}\,z + a\,,$$

where the derivatives and the a function are taken at point $(0,0,0)$. Let us find the average value of a at a distance δ from the point $(0,0,0)$, understanding it as

$$\langle a_\delta\rangle = \frac{1}{6}\big[a(\delta,0,0) + a(-\delta,0,0) + a(0,\delta,0) + a(0,-\delta,0) + a(0,0,\delta) + a(0,0,-\delta)\big]\,.$$

Then we arrive at

$$a(\delta,0,0) + a(-\delta,0,0) = \frac{1}{2}\frac{\partial^2 a}{\partial x^2}\,\delta^2 + \frac{\partial a}{\partial x}\,\delta + a + \frac{1}{2}\frac{\partial^2 a}{\partial x^2}\,\delta^2 - \frac{\partial a}{\partial x}\,\delta + a = \frac{\partial^2 a}{\partial x^2}\,\delta^2 + 2a\,.$$

Expressions for $a(0,\delta,0) + a(0,-\delta,0)$ and $a(0,0,\delta) + a(0,0,-\delta)$ are obtained similarly.

Substituting these expressions into $\langle a_\delta\rangle$, we find

$$\langle a_\delta\rangle = \frac{1}{6}\left(\frac{\partial^2 a}{\partial x^2} + \frac{\partial^2 a}{\partial y^2} + \frac{\partial^2 a}{\partial z^2}\right)\delta^2 + a = \frac{1}{6}\,\delta^2\nabla^2 a + a\,.$$

Hence follows

$$\frac{\nabla^2 a}{a} = 6\,\frac{\langle a_\delta\rangle - a}{a\delta^2}\,. \tag{2.6}$$

Therefore, the quantity given by formula (2.6) shows how much the field at the center is weaker than the field in the nearest neighborhood. This quantity will be further called the **rarefaction** of the quasifield.

Note that the rarefaction is independent of the field intensity. It is also independent of the rotation of coordinate axes, since, as we know, $\nabla^2 a$ is independent of it.

In Eqn (2.5), the first term in the expression for the acceleration of the quasifield and the T-particle is directed along the rarefaction gradient of the quasifield towards larger rarefactions and is proportional to the gradient. Therefore, the quasifield will tend to move in such a way that the rarefaction will be reduced and spread uniformly over space.

Since the velocities of travel of the quasifield elements are determined, according to Eqn (1.8), by a gradient of the scalar β, then $\operatorname{rot}\mathbf{V} = 0$, i.e., the quasifield cannot have any vortices.

2.5 As we have already mentioned, the state of an elementary particle is fully determined by its wavefunction (1.1). This wavefunction also fully determines the parameters of the quasifield, such as its density a^2 and velocity of travel $\mathbf{V} = (\hbar/m)\nabla\beta$. However, the inverse is not true: it is impossible to fully determine the wavefunction knowing only the density and the velocity of the quasifield. Indeed, in this case we will only know, according to Eqn (1.8), the modulus of the wavefunction and the gradient of its argument, i.e., the derivatives of the argument with respect to the coordinates. Moreover, one can add to the argument an arbitrary function of time, which is independent of the coordinates, and the gradient will not change.

In order to define β, one should also know the derivative $\partial\beta/\partial t$. It can be found from equation (1.7), provided that U is known, since the wavefunction should satisfy the Schrödinger equation. Then we obtain

$$\beta(\mathbf{r},t) = \beta(\mathbf{r}_0,t_0) + \int_{t_0}^{t}\frac{\partial\beta(\mathbf{r}_0,t)}{\partial t}\,\mathrm{d}t + \int_{\mathbf{r}_0}^{\mathbf{r}}\nabla\beta(\mathbf{r},t)\,\mathrm{d}\mathbf{r}\,. \tag{2.7}$$

Thus, the quasifield, in combination with U, determines the wavefunction up to a constant $\beta(\mathbf{r}_0,t_0)$, which has no effect on the state of the quanton.

Similarly to the way in which not every complex function can be a wavefunction, since it has to satisfy the Schrödinger equation, not every field $a^2(\mathbf{r}, t)$ and $\mathbf{V}(\mathbf{r}, t)$ can represent a quasifield: they have to correspond to some wavefunction.

2.6 If we substitute the wavefunction $\psi(\mathbf{r}, t) = a(\mathbf{r}, t)\exp\big(\mathrm{i}\beta(\mathbf{r}, t)\big)$ into Schrödinger equation (1.3) and take into account relation (2.3) for the quasifield velocity, then expressions (1.6) and (1.7) for the real and imaginary parts of the Schrödinger equation acquire a simple physical meaning. Indeed, with account for Eqn (2.3), relation (1.6) becomes

$$\frac{\partial a^2}{\partial t} = -\nabla(a^2\mathbf{V}), \tag{2.8}$$

and relation (1.7), if one takes the gradients of both its sides, changes to

$$-m\,\frac{\partial \mathbf{V}}{\partial t} = -\frac{\hbar^2}{2m}\,\nabla\,\frac{\nabla^2 a}{a} + \frac{m}{2}\,\nabla V^2 + \nabla U. \tag{2.9}$$

Equation (2.8) is equivalent to equation (2.2) and indicates that the quasifield cannot appear or disappear but can only be displaced. Equation (2.9), taking into account Eqns (1.10) and (2.3), will be equivalent to Eqn (2.5), i.e., to the statement that acceleration of the quasifield elements is equal to the sum of the forces, the external one and the quasifield one, divided by the particle mass. Thus, the Schrödinger equation for the quasifield corresponds to the gas dynamics equation, the only difference being that the force of the quasifield self-action, denoted here by $\mathbf{F}_{\mathrm{q}}$, is essentially different from the analogous force in gas dynamics.

PACS numbers: **01.65.+g**, **95.55.−n**, **96.30.−t**
DOI: 10.3367/UFNe.0179.200902i.0208

Vladimir Aleksandrovich Kotel'nikov and Solar System studies

L M Zelenyi, N A Armand

1. Introduction

In biographically portraying the work of Academician Vladimir Aleksandrovich Kotel'nikov, one usually describes his outstanding work devoted to the fundamentals of the communication theory (the famous sampling theorem, the potential noise immunity theory, theorems in cryptography theory). His role in Soviet space programs is described to a lesser extent. Meanwhile, the contribution of Vladimir Aleksandrovich and colleagues from the organizations founded and headed by him [the Special Design Bureau of Moscow Power Engineering Institute (OKB MEI in *Russ. abbr*.) and the Institute of Radioengineering and Electronics of the Russian Academy of Sciences (IRE RAS)] to this field is also very significant. Another side of his 'space' activity is related to his positions as the Vice President of the USSR Academy of Sciences and the Head of the Intercosmos Council.

In this short report we shall briefly describe the main stages of V A Kotel'nikov's activity, who was an outstanding scientist, engineer, politician, and scientific manager.

2. V A Kotel'nikov and space radar

The development of space radar was motivated by quite practical needs. In the 1960s, the state of space facilities in the USSR and USA allowed scientists and engineers to plan scientific space missions in order to explore nearby planets: Venus and Mars. To ensure the approach of spacecraft to these planets at a distance of several hundred kilometers, one needed to know their position relative to Earth with a good accuracy. Previous astronomical observations of Solar System's bodies located them precisely only relative to each other, while the absolute values of the mutual distances had been known very crudely from the space navigation point of view, which required high accuracy to handle the spacecraft.

All distances between planets are conveniently expressed through the astronomical unit (a.u.), which is equal to the mean distance from Earth to the Sun and is estimated to be around 150 mln km. Astronomical observations had determined this value to an accuracy of about 10,000 km. This means that the distance, for example, to Venus had been known to an accuracy of several thousand kilometers. Clearly, this accuracy could not be considered as satisfactory.

Radio ranging provided the possibility of measuring the distance between Earth and a nearby planet with the required accuracy. To measure the distance with a one-kilometer accuracy, it is sufficient to send radio pulses with a duration of approximately 6 μs. The question is how powerful these pulses should be for the reflected signal to exceed the noise level in a ground-based detector. Considering that in radio ranging 'the inverse fourth power distance law' operates and interplanetary distances are at best several dozen million kilometers, it is easy to understand that antennas with an area of several thousand square meters and transmitters with a power of several dozen kilowatts are required for successful radio ranging of planets. This was very expensive and accessible only for countries with highly developed industry. So it was quite natural that planetary radar started developing in the USA, the USSR and partially in the UK.

At that time, the Remote Space Communication Center (RSCC) was constructed near the city of Eupatoria (Crimea) in the USSR. The center was designed for communications primarily with spacecraft to be sent to Venus and Mars. For this purpose, three ADU-1000 antennas (Fig. 1) were constructed: one for signal transmission, and the other two for signal reception. The radio transmitter with a power of about 10 kW operated at a wavelength of 40 cm. These characteristics fit planetary radar requirements, so the RSCC was chosen to perform the experiment.

Advances in radar facilities (increase in transmitter power and detector sensitivity, development of digital frequency-linear signal modulation, etc.) allowed a very precise measurement of the astronomical unit: 1 AU $=$ 149,597,867 $\pm$ 0.9 km. Such an accuracy required knowing very precisely the speed of light, since in radio ranging one directly measures the time of radio pulse propagation, and the distance between space bodies is obtained by multiplying the delay time by the speed of light. For this reason, the XVIth General Assembly of the International Astronomical Union (1967), by analyzing the results of experiments carried out in the USSR and USA, adopted the value of 1 AU $=$ 149,597,870 $\pm$ 2 km for the assumed speed of light $c =$ 299,792,558 $\pm$ 1.2 m s^{-1}. Such a high accuracy in determining the astronomical unit has provided successful flights of spacecrafts for planetary studies and exploration of the interplanetary space in the Solar System. Moreover, such an

Figure 1. The ADU-1000 antenna.

V A Kotel'nikov with colleagues from the Institute of Radioengineering and Electronics, who participated in Venus radar ranging. (From left to right: A M Shakhovskii, V A Kotel'nikov, O N Rzhiga, V M Dubrovin.)

Figure 2. The TNA-2500 antenna.

accuracy required the usage of general theory of relativity for the correct description of motion of the Solar System planets. This problem was tackled, in particular, thanks to efforts of specialists from the Central Research Institute of Mechanical Engineering (TsNIIMASh in *Russ. abbr.*), the Institute of Applied Mathematics (IAM) RAS, and IRE RAS.

In addition to determining the astronomical unit by means of planetary radio ranging, other interesting results have also been obtained. Let us discuss the most important result in our opinion, which is related to the determination of the rotational period of Venus. It was very difficult to determine this period by optical methods since Venus is covered by a thick cloudy layer. Radar methods afforded the possibility of determining the planet's rotational period, since the rotation produces spectral broadening of the radio signal reflected from the planetary surface. As a result, the rotational period of Venus was found to be $T = 243.04$ days, which was about the same value as obtained in the USA. The International Astronomical Union adopted this period to be 243.01 days. It is interesting to note that in contrast to other planets, Venus has the opposite rotation with respect to the sense of orbital revolution around the Sun. Interestingly, the measured value is very close to the period of synodical resonance at which only one side of Venus should have been observed from the Earth at periods of the bottom conjugation.

The experience of planetary radar accumulated by IRE RAS was broadened by pupils of Vladimir Aleksandrovich during radio ranging of small bodies of the Solar System. These bodies having small sizes, the bistatic ranging method turned out to be the most convenient, in which the illumination was performed by one antenna and the reception of the reflected signal was made by another antenna. When the radars are located sufficiently far away from each other, it is possible to emit quite a long-duration signal and coherently accumulate the reflected signal with the receiving antenna. This required international collaboration, in which financial consideration also played its role. The Russian side, more precisely, the Russian – Ukrainian side, used the TNA-2500 antenna (Fig. 2) constructed at CRSC (in the city of Eupatoria) as far back as in the Soviet times. Foreign collaborators used antennas at Effelsberg (Bonn), at Goldstone (USA), at Kashima (Japan), and at Medicina (Italy). The following asteroids were radio ranged: 4179 Tautatis, 6479 Golevka, and 1998 WT24. The analysis of the received signals allowed estimation of the rotational velocity of these objects, their sizes, the scattering capability, etc. Figure 3 demonstrates the possibilities of spectral analysis for reconstructing the surface relief of the WT24 asteroid. When reconstructing the relief, the permanent rotation of the asteroid is essential, so that radio waves scattered by different points of its surface experience different Doppler shifts. The total spectrum of the scattered signal is similar to the spectra shown in the left panel of Fig. 3 for two orthogonal circular polarizations obtained for different aspect angles of the asteroid.

Space planetary radar was further developed with the launch of the Venera-15 and Venera-16 missions that had onboard radars with a synthesized aperture. As mentioned

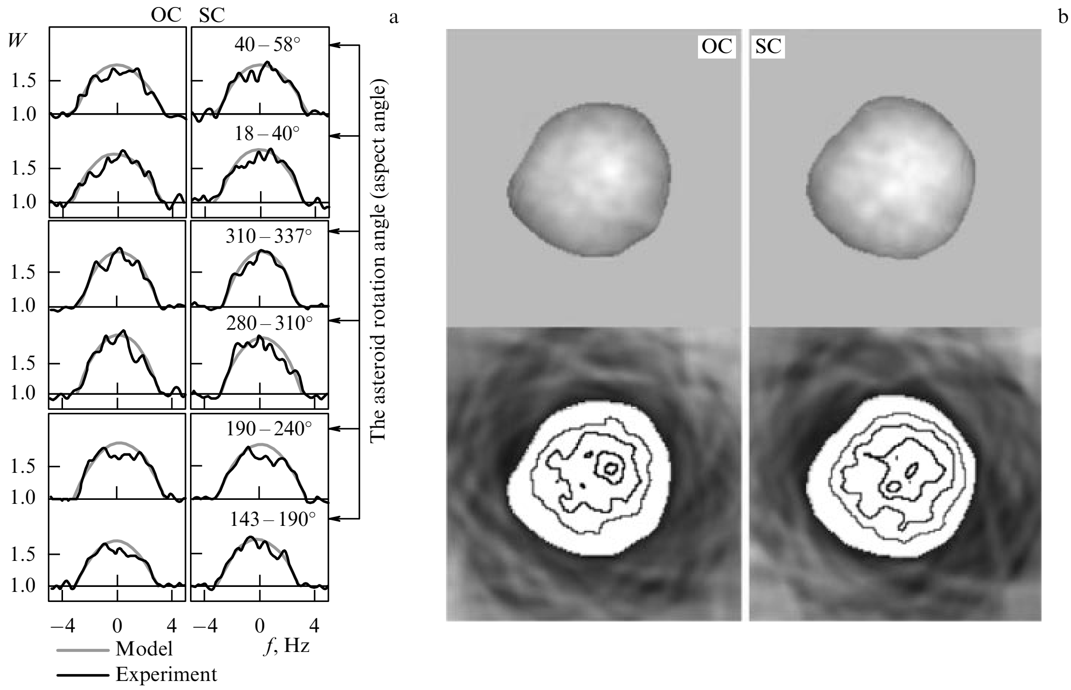

Figure 3. (a) Comparison of the observed and model power spectra from a rough ellipsoid observed at different aspects. (b) Radio image of the asteroid WT24 in two polarizations.

above, the surface of Venus is permanently covered by a thick cloudy layer, so it is impossible to capture its image in the optical range even from the planet's artificial satellite. It could be done only by a planetary lander, which was accomplished in 1975 by the Venera-9 and Venera-10 spacecraft. Here one should take into account that the landers operated under a temperature of about 700 K and a pressure of about 100 atmospheres. But the area of the surface observed by these modules was too small to make meaningful geological conclusions; this requires imaging large areas, which can be done only from satellites of the planet.

This task was successfully realized in 1983 by the Venera-15 and Venera-16 missions. Radars with a synthesized aperture on these satellites (Fig. 4) allowed taking images of the planetary surface from a distance of 1000 km with a spatial resolution of 1 km.

V A Kotel'nikov was the informal leader of this project and played the decisive role in coordinating the activity of IRE RAS, OKB MEI, Lavochkin Research and Production Association, and several other industrial and academic organizations. The imaging of 115 mln km^2 of the north Venerian hemisphere (25% of the planetary surface) was done. An example of one of such radar images is shown in Fig. 5.

The radar imaging of a planet fully covered with clouds was an outstanding scientific achievement that greatly contributed to world science. The analysis of these images has been invaluable for the development of comparative planetology.

The realization of this project also contributed to the development of the radar image processing technique. In particular, for the first time in the Soviet Union the procedure for obtaining digital images was carried out. This experience was later applied in designing the software for processing radar images taken by radars with synthesized aperture onboard the Almaz orbital complex, designed for performing radio cartography of the surface of the Earth with a spatial resolution of 10 m.

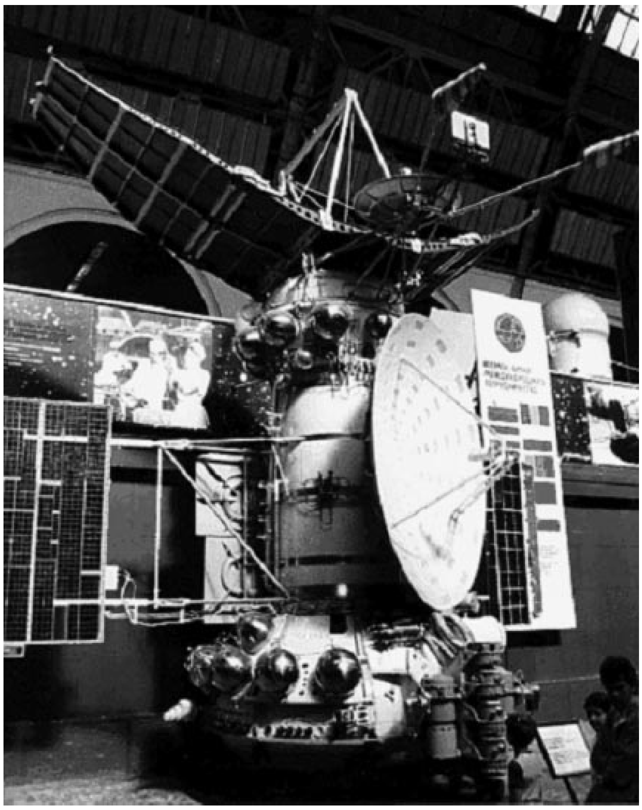

Figure 4. The Venera-15 spacecraft.

Prospects for Solar System radio ranging research. Radar studies of the planets of the Solar System initiated under the leadership of V A Kotel'nikov was continued in IRE RAS

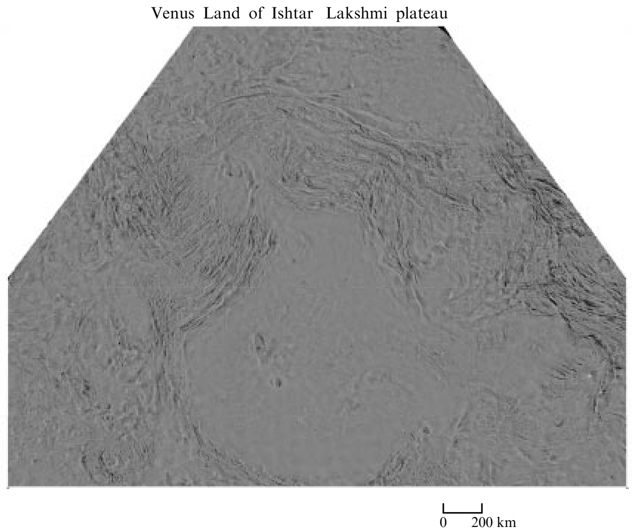

Figure 5. A portion of a radar image of Venus.

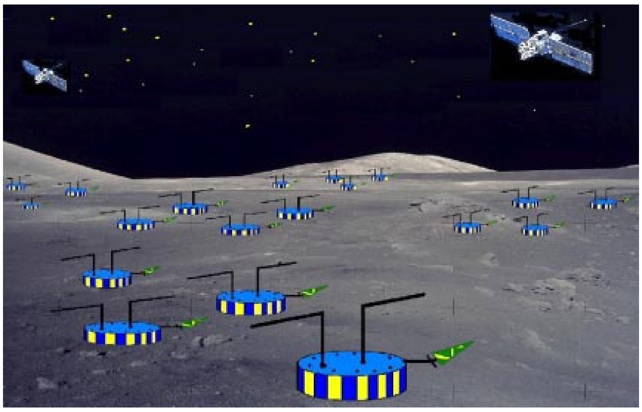

Figure 6. Low-frequency radio astronomy on the lunar surface.

programs aimed at the subsurface radar sounding of the planets realized from their artificial satellites. Currently, these studies are being carried out at the stage of processing the data obtained with the MARSIS radar (Mars Advanced Radar for Subsurface and Ionosphere Sounding) onboard the Mars-Express spacecraft launched by the European Space Agency (ESA).

Radar studies in the framework of the Phobos-Ground project are in prospect. It is planned to install onboard a module landing on the surface of Phobos a subsurface-sounding radar operating at a carrying frequency of 150 MHz with a bandwidth of 50 MHz. It is assumed that this module will probe the subsurface structure of Phobos up to depths of at least 100 m with a resolution of 2 m.

The possibility of subsurface radio ranging of the Moon is also being discussed (Fig. 6). The principal tasks include:

- studies of the subsurface layer structure up to a depth of several kilometers;
- studies of the dielectric properties of the lunar ground;
- discovery and identification of large inclusions of various rocks;
- localization of ground sites with enhanced passability;
- studies of large-scale lunar roughness;
- improvement of the lunar surface topography.

To address these issues, it is required to design a multi-frequency radar with final specifications according to the detailed Russian program of lunar studies, which is now under formation.

In a long-term outlook, radar imaging of the icy sheath of the Jovian satellite Europa (with the estimated bulk from several kilometers up to 100 km) is feasible. If this ice is freshwater, it is virtually transparent in a wide radio frequency range. So, the dielectric properties of the icy sheath are essential for the choice of radar frequencies. For example, due to large scattering on the highly rough ice, too short radio waves (e.g., of decimeter wavelengths) cannot be used. Decameter waves cannot also be chosen because of the strong noise generated by synchrotron radiation in the Jovian radiation belts. Apparently, using meter wavelengths could be the compromise. Time will show what the choice of the Russian space mission towards Europa will be. However, the strong level of radioactivity around Jupiter is the most severe problem. This places high demands on the safety of both the space platform and its service and scientific payload. This also leads to a significant shortening of the entire lifetime of the mission.

3. V A Kotel'nikov and the Intercosmos program

Space research and explorations require international collaboration. It should be recalled that the first artificial satellite of the Earth (ASE) was launched during the International Geophysical Year (1957 – 1958) — a wide program of terrestrial studies, in which scientific institutes from 66 countries were involved.

The First Secretary of the Central Committee of the Communist Party of the Soviet Union (CC CPSU) at that time, Nikita Khrushchev, very rapidly (only in a few days after the launch of the first ASE) became aware of a huge propaganda potential of space research due to the frequently hidden military implications of civil explorations.

It was also obvious that science, including rapidly developing space research, could become a powerful addition to economic successes, and a means of strengthening the relations (both ideological and personal) between peoples from socialist countries. Nuclear physics and space research seemed to be the most important fields of science in the second half of the 20th century. Quite rapidly, without the usual red tape, the Joint Institute for Nuclear Research in Dubna and the Council for International Collaboration for Space Research and Exploration of the USSR Academy of Sciences (the Intercosmos Council, for brevity) were founded under the leadership of the Vice President of the USSR AS, Academician B N Petrov.

Space physics, space meteorology, the physics and techniques of remote radio communications and television, space biology and medicine, and distant Earth sounding (DES) were to become the principal fields of scientific collaboration in space research.[1] The joint construction and launching of artificial satellites and the design of equipment and scientific payload were also being discussed.

By April 1967, the detailed program of joint space research has been elaborated. The program involved institutions from Bulgaria, Hungary, Vietnam, the GDR, Cuba, Mongolia, Poland, Romania, the Soviet Union, and Czechoslovakia. The scientific potentials of these countries were very different, and the motto of Intercosmos, "Socialism is the

[1] DES was added to the program in 1973.

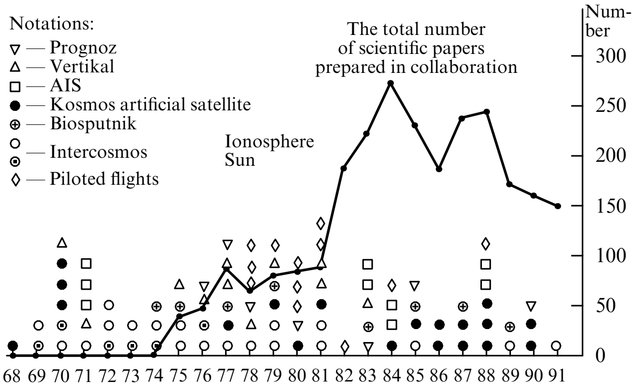

Figure 7. History of the Intercosmos space launches.

launch pad for space flights,'' can be remembered now both ironically and with a certain nostalgia. But that was our past, and the above words were to a large extent correct — exactly at that time the space industry was founded in the countries participating in the Intercosmos program.

We stress from the very beginning that the Soviet Union provided other countries participating in the Intercosmos program with free access to all Soviet technology, unique at that time, including spacecraft, rockets, launch sites and ground measurement stations, and equipment for preparing, launching, and controling the space flights. Another feature of the Intercosmos program was that each country proposed its own research program and could participate in partners' experiments which were of interest to it, in designing the scientific payload, and, frequently, in the elaboration of service systems to be installed onboard satellites; the results of joint research were equally shared among the participants.

At the annual meetings the leaders of national coordinating bodies took principal decisions, issued recommendations concerning different practical problems, and discussed the prospects of cooperation developing in different fields. In 1980, the outstanding Soviet scientist and science administrator V A Kotel'nikov became the head of the Soviet national coordination body and Head of the Intercosmos Council. Under his leadership in the 1980s, the program matured and the most significant scientific research was carried out (Fig. 7).

The first step in pursuing the Intercosmos program was the realization of a space experiment on complex studies of the upper terrestrial atmosphere and the nature of aurora, conducted onboard the Kosmos-261 satellite in December 1968.

The complex experiment was prepared jointly by research institutes and geophysical observatories from the countries participating in the Intercosmos program. Synchronous ground-based observations of the atmosphere and troposphere had been organized and the obtained space and ground-based data were jointly analyzed. Several new results were obtained, in particular, the diffusion of the auroral zone toward the equator from the oval of discrete auroras was discovered.

Simultaneously, new satellites for further research were being elaborated. In the technical documentation of the Yuzhnoe Design Bureau in Dnepropetrovsk, these satellites were named Intercosmos-1, Intercosmos-2, etc. And although the Kosmos-261 satellite (by the way, the first practical work of plasmophysicists from the Space Research Institute of the USSR AS that was founded shortly before) officially opened the Intercosmos program, it was decided not to change its name in order not to confuse drafts and documentation.

On October 14, 1969, the Kosmos-1 launch vehicle (the converted version of the R-12 ballistic missile) put into orbit the spacecraft D-UZ-IK-1, called by the press Intercosmos-1. The launch took place in the Kapustin Yar launch site (about twenty kilometers from Volgograd) in the presence of scientists from nine countries participating in the program.

In the following years, in the framework of the Intercosmos program 24 other satellites of the Intercosmos series were launched, 11 high-altitude Vertikal rockets and several hundred meteorological rockets of different modifications. In total, from 1967 to the beginning of the 1990s, taking into account scientific and social-economic spacecraft (biosatellites, Meteor, Meteor-Priroda, Molniya, etc.), automatic interplanetary stations (AISs) Luna, Venera, Vega, etc., piloted Soyuz spacecraft and orbital stations (Salyut, Mir series), the well-developed missile and space infrastructure of the USSR in collaboration with participating countries of the Intercosmos program allowed around 100 spacecraft with various destinations (excluding meteorockets and high-altitude balloons) to be launched.

Most Intercosmos satellites (22 of 25) were manufactured in the Yuzhnoe Design Bureau under the leadership of V M Kovtunenko. In order to design and organize in a short period of time the industrial production of a large number of spacecraft of different destinations, nonstandard decisions were required. The principle of base platform unification (i.e., the usage of a unique frame structure, the standard set of service units, a common scheme of payload control, a common system of electric power supply) turned out to be the most acceptable. For the first time in the world, in essence, line production of satellites was organized. The unification allowed not only shortening the manufacturing time, but also significantly decreasing the production costs.

Starting from Intercosmos-15, a more complex and heavier platform — the automatic unified orbital station (AUOS) — was utilized. To put this platform into orbit, a more powerful launch vehicle was required — the conversion variant of the R-14 ballistic missile. During the flight of Intercosmos-15 new onboard systems were also tested, including the united telemetric system (UTMS) elaborated jointly by specialists from Hungary, the GDR, Poland, the USSR, and Czechoslovakia. This system allowed the telemetry from satellites to be received by ground stations located in the territory of the participating countries. The UTMS was also installed onboard the next Intercosmos-18 and Intercosmos-19 satellites.

The Intercosmos satellites, depending on their destination and scientific goals, can be subdivided into several groups, including:

• Solar series: Intercosmos-1 (1969), Intercosmos-4 (1970), Intercosmos-7 (1972), Intercosmos-9 (Copernicus-500) (1973), Intercosmos-11 (1974), and Intercosmos-16 (1976). These satellites were designed to study ultraviolet and X-ray solar radiation and sporadic solar radio emission;

• ionospheric series: Intercosmos-2 (1968), Intercosmos-8 (1972), Intercosmos-12 (1974), Intercosmos-19 (1979), Intercosmos-22 (Bulgaria-1300) (1981);

• magnetospheric series: Intercosmos-3 (1970), Intercosmos-5 (1971), Intercosmos-6 (1972), Intercosmos-10 (1973), Intercosmos-13 (1975), Intercosmos-14 (1975), Intercos-

Figure 8. The Intercosmos-20 spacecraft.

mos-17 (1977), Intercosmos-18 (1978). These satellites were designed to study processes in the upper terrestrial atmosphere, low-frequency electromagnetic radiation, the dynamics of terrestrial radiation belts, ultrahigh-energy cosmic radiation, and electromagnetic coupling between the magnetosphere and ionosphere. Intercosmos-6 satellite was equipped with a lander with a scientific payload.

The small Czechoslovakian satellite Magion was separated from Intercosmos-18. The joint flight of two spacecraft was aimed at studying the spatial structure of low-frequency electromagnetic fields in near-Earth space. Coordinated observations were carried out from ground-based ionospheric and solar observatories of the countries participating in the program.

Testing of an experimental system of data acquisition from ground-based and naval measuring facilities (buoys) and its retransmission through the central station to customers was started onboard the Intercosmos-20 and Intercosmos-21 spacecraft (Fig. 8). For the first time, the multizone spectrophotometer MKS was installed onboard these satellites. This device successfully combined the scientific methods developed by Soviet scientists and the technical facilities produced by specialists from the GDR. The updated variant of this instrument later operated onboard the Salyut-7 piloted orbital station.

Intercosmos-22, devoted to the 1300th anniversary of the Bulgarian state foundation, was constructed by Bulgarian and Soviet specialists. The scientific payload included a multichannel optical electrophotometer, a high-energy ion and electron analyzer, an ion drift meter, an ultraviolet photometer, units to measure electron temperature and number density, a unit to measure the ionic component of plasma, a proton counter, an ultrahigh frequency radiometer operating at a wavelength of 4 cm, and some other devices. The Meteor-2 spacecraft was chosen as the base platform for this satellite.

In April 1985, Intercosmos-23 (also known as Intershock) was launched which, like Intercosmos-1, -4, -7, -9, -11, and -16, was designed to study solar–terrestrial relations. In this case, studies were carried out on a new basis, from the Prognoz automatic station (Fig. 9). The orbit of this satellite was elongated toward the Sun and reached several hundred thousand kilometers in the apogee. This allowed probing regions outside terrestrial magnetic field during most of the orbital period. The launch was aimed at studying the structure of the interplanetary and near-Earth shocks produced by solar wind interaction with the Earth's magnetosphere. Such shocks have an unusual structure, since particle collisions (which lead to braking the hypersound fluxes in ordinary gases) are nearly absent in extremely rarefied space plasma, and the necessary dissipation is provided by collective wave processes. The station was equipped with devices elaborated by scientists from the USSR and Czechoslovakia. Another feature of Intercosmos-23 (Prognoz-10) (Fig. 10) was the presence of various rapidly operating diagnostic tools, including a multichannel plasma spectrometer and a complex of devices measuring plasma waves, as well as an onboard computer controlling the experiment and providing automatic measurement of the shock front crossing time,

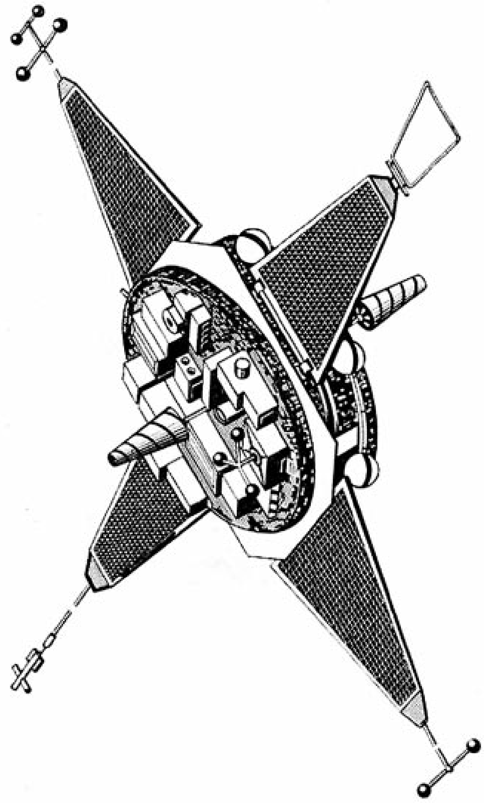

Figure 9. The base platform — the Prognoz station.

Figure 10. Intercosmos-23 (Prognoz-10).

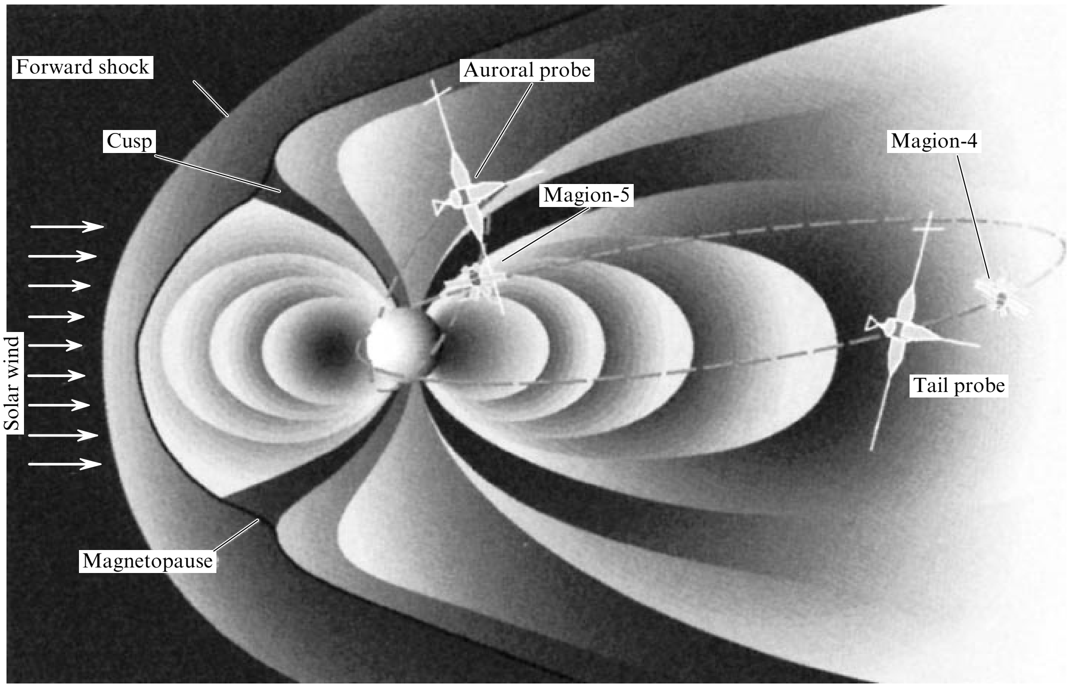

Figure 11. The Interbol project.

which enabled rapid data storage exactly near the front. There was also a ring memory to store the prehistory of the shock crossing.

Due to the complex approach to carrying out the research, the measurement of all necessary and, most of all, key characteristics of the studied processes, the possibility of 'teaching' the onboard devices, and the flexibility in building the program of measurements and their high time resolution at the shock crossing instant, the internal structure of shock front was studied and the physical processes responsible for shock formation, as well as particle acceleration and heating were identified. A deeper insight into the process of ion thermalization in supercritical shock waves due to their front instabilities has been one of the important results of this research.

It is worth remembering that V A Kotel'nikov was personally interested in the results of experiments performed by Intercosmos-23 and actively supported at all stages the realization of this complex program of collisionless shock studies.

Intercosmos-24, launched in September 1989, became one of the first perestroika scientific satellites. Its distinctive feature compared to other satellites of this series has been scientific data acquisition, not only in the Intercosmos collaboration countries, but also in the USA, Brazil, Canada, Finland, Japan, and New Zealand.

The goal of the launch was complex research of very low-frequency (VLF) electromagnetic wave propagation in the Earth's magnetosphere and the waves' interaction with fast charged particles in the radiation belts. An active experiment was also planned to study VLF-wave propagation in the Earth's magnetosphere and magnetospheric plasma processes, hence the name of the project — Aktivnyi (Active).

Intercosmos-24 had to significantly enlarge information available at that time on the plasma shell of the Earth located at altitudes from 100 to 500,000 km and its interaction with the Earth's magnetosphere. Scientists counted on estimating the effects of many processes on the near-Earth plasma: generation of magnetic storms influencing human health, aurora particle drop-out, the effect of many radio transmitters producing a radiohalo around the Earth, lightning discharges, etc.

For more precise and detailed studies of wave processes, the Magion-2 subsatellite constructed in Czechoslovakia had to be operated in tandem with Intercosmos-24. The scientific payload of both satellites was designed in the Soviet Union, Hungary, Bulgaria, Czechoslovakia, the GDR, Poland, and Romania. It was planned that the subsatellite, after detaching from the main satellite, would be flying for several months immediately close to it (at a distance from several meters to 10 km). Unfortunately, a failure in the engine device and the VLF-generator did not allow the full performance of the program.

Shortly after the launch of Intercosmos-24 in 1989, the intention to start active research of the plasma shell around the Earth was declared. For this purpose, the project Aktivnyi-2 was planned to be realized in the first half of the 1990s. In 1990, this project was officially given a new name APEX (Active-Plasma Experiment). The project was aimed at studying the influence of modulated electron and plasma beams on the terrestrial ionosphere and magnetosphere. During the experiment, it was planned to estimate electric fields and currents mediating the ionosphere–magnetosphere interaction, as well as to assess charged particle fluxes along the field lines of the geomagnetic field. The measurements had to be carried out by the Intercosmos-25 satellite, which scientific payload partially included a replica or an upgrade of the Intercosmos-24 devices.

The satellite was launched in December 1991. In 10 days, the microsatellite Magion-3, manufactured by the Czech Republic and Slovakia, separated from the basic spacecraft. Its scientific payload allowed taking measurements of almost the same physical quantities as the main satellites. This time the sub-satellite had no correcting engine, and keeping it at a distance of ten to a hundred meters was provided by the engine device of the primary satellite.

Intercosmos-25 successfully obtained many interesting results. All scientific units operated normally. A series of active experiments on studying emission from plasma and electron beams and their detection was carried out by the subsatellite.

In the 1990s, after the dissolution of the Soviet Union, the organizational structure of the Intercosmos Council was de jure dissolved. The Council for Mutual Economic Assistance, the Warsaw Pact ceased to exist. In most of the countries participating in the Intercosmos program, the economical and political regimes changed, but scientific and personal relations between scientists have persisted.

One of merits of the Intercosmos program was the increasing from year to year internationalization of Soviet cosmonautics. For example, in the Vega (Venus–Galley) project realized in 1984, in addition to the countries permanently collaborating on the Intercosmos program, scientists from Austria, Germany, and France participated in the manufacturing of the scientific payload installed on automatic interplanetary stations Vega-1 and Vega-2.

The first part of the flight program of these stations was aimed at exploring the atmosphere and surface of Venus. To this effect, balloon-borne probes were used for the first time. During the second part of the program, the stations approached the Galley comet and after 450 days of flight, in March 1986, they passed near the comet's core at a distance of about 10,000 km. In the experiments, the size and form of the cometary core were determined along with the surface properties and the temperature and chemical composition of the gas, dust, and other parameters of the comet. In addition, television pictures of the comet were recorded and transmitted to Earth.

Planetary projects Phobos and Mars-96 and astrophysical missions Kvant and Spektr series were prepared under a broader international cooperation.

The Intercosmos program was in fact continued in the middle of the 1990s during the realization of the largest international project, Interbol (Fig. 11), in which 14 countries participated. The project became a part of a broad international program coordinated by the Inter-Agency Consultative Group (IACG), including representatives of the ESA, NASA, the Russian Space Agency, and the Institute of Space and Aeronautical Science (Japan).

The Interbol multisatellite project became one of the most successful missions aimed at the studies of physical processes in near-Earth space during the whole history of solar–terrestrial relations research in the Soviet Union and Russia. During the realization of this project, a system consisting of two pairs of satellites was constructed and realized: the primary satellite, Interbol-1, with subsatellite Magion-4, and the subsidiary satellite Interbol-2 with subsatellite Magion-5. This setup allowed making simultaneous measurements in different parts of the Earth's magnetosphere and enabled the separation of spatial and time variations of the measured parameters.

The Interbol project collected the unique (in significance, volume, and quality) experimental material. It became possible first of all due to much more extensive data transmission capacity from the spacecraft to the ground compared to the previous Prognoz series, and to simultaneous multisatellite observations from both close and remote distances in the Earth's magnetosphere. The lifetime of the satellites was much longer than their assured life. These factors were crucial for providing a high scientific level of the results obtained. The results of the conducted research were published in more than 500 papers diverse in themes and approaches to the analysis of measurement results.

During the realization of this project, new important data had also been obtained on the long-term impact of different space factors on the onboard payload and functionality of technical systems, which yielded valuable recommendations for developers of space technologies.

Presently, several new large international space projects are under preparation. The impetus given by the Intercosmos program and personally by V A Kotel'nikov was crucial for surviving the hard times of the 1990s and, despite the political woes, for preserving and continuing scientific collaboration with colleagues from Eastern and Western Europe at a new and higher level. Now full scientific collaboration in space has been restored with Poland, Bulgaria, and France. A new agreement with the Czech Republic is under preparation.

The experience of Intercosmos turned out to be also very important in establishing relations with CIS countries.

The authors acknowledge Yu I Zaitsev and V S Kornilenko for the help in the preparation of the text of the report for publication.

PACS numbers: **01.65.+g**, **02.70.–c**, **89.70.–a**
DOI: 10.3367/UFNe.0179.200902j.0216

Development of Kotel'nikov's sampling theorem

N A Kuznetsov, I N Sinitsyn

1. Introduction

The name of Academician V A Kotel'nikov means a full epoch in the development of communication systems, radio engineering, and radiophysics. His greatest research achievements had a considerable impact on scientific progress throughout the world. Among them, one should mention his *sampling theorem* [1], the theory of potential noise immunity, which provided scientists and engineers with an instrument for the synthesis of optimal systems for signal processing in communication systems, radar, radio navigation, and other fields, and finally, the development of planetary radars admitting of basic astronomic research with their help.

In 1932, Kotel'nikov prepared a conference report, "On the transmission capacity of 'ether' and wire in electric communications." In this report, he gave the first formulation of the famous sampling theorem, one of the basic theorems in communication theory. This report was published, as a small edition, in 1933.

Let us consider below recent developments of the sampling theorem, its relation to the filtering of continuous signals using discrete observations, and the informational aspects of numerical simulation in the digital processing of complex signals.

2. Kotel'nikov's sampling theorem

Sampling theorem in the time domain. *A continuous signal $x(t)$ whose spectrum is limited by a maximal frequency F_{m} can be unambiguously and losslessly restored from its discrete samplings taken with a rate of $F_{\mathrm{discr}} \geqslant F_{\mathrm{m}}$. The algorithm of* *interpolating this signal from discrete samplings spaced at Δt_{m} time intervals is given by*

$$x(t) = \sum_{k=-\infty}^{\infty} x(k\Delta t_{\mathrm{m}}) \frac{\sin\left[\omega_{\mathrm{m}}(t - k\Delta t_{\mathrm{m}})\right]}{\omega_{\mathrm{m}}(t - k\Delta t_{\mathrm{m}})}, \tag{1}$$

where $\omega_{\mathrm{m}} = 2\pi F_{\mathrm{m}}$ is the Kotel'nikov frequency. The sampling interval $\Delta t_{\mathrm{m}} = 1/(2F_{\mathrm{m}})$ is often termed the Kotel'nikov interval.

Sampling theorem in the frequency domain. *For a signal $x(t)$ limited by time $|t| < T$, its continuous spectrum $s_x(f)$, is represented as*

$$s_x(f) = \sum_{k=-\infty}^{\infty} s_x(2\pi k\Delta f) \frac{\sin 2\pi T(f - k\Delta f)}{2\pi T(f - k\Delta f)}, \tag{2}$$

where Δf is the frequency sampling interval.

Independently, the sampling theorem was discovered in 1949 by the outstanding American scientist C Shannon, who was the founder of the information theory, an important part of the communication theory. This theorem was extremely valuable for communication technology. It is worth noting that as a special mathematical result of the function interpolation theory, this theorem had been formulated as early as the beginning of the 20th century by British mathematicians E T Whittaker and J M Whittaker. However, this great scientific achievement is rightly attributed to the names of Kotel'nikov and Shannon, since it is only their discovery of the sampling theorem that enabled engineers to develop digital systems, which later in the 20th century made a revolution in electric communications and digital signal processing.

3. Applications of Kotel'nikov's theorem

Kotel'nikov formulated the sampling theorem trying to answer the following principal question: What minimal bandwidth is required for transmitting through a communication channel a signal whose spectral band is strictly limited? Today, this theorem is generally recognized as one of the fundamental results of digital signal processing (DSP) in the communication theory.

The theorem has an extremely broad field of applications. As an example, let us mention discrete communication channels and devices for digital information writing, aimed at the transmission and recording of acoustic signals. According to Kotel'nikov's theorem, the following sampling rates have been chosen:

- 8000 Hz for the telephone;
- 22,050 Hz for radio;
- 44,100 Hz for the audio CD.

Broad application of these devices is evident from the fact that in 2003, according to the Recording Industry Association of America (RIAA), 749.9 million CDs were sold.

4. Generalizations of Kotel'nikov's theorem

The design and exploitation of new digital devices for recording, transmitting, and reproducing continuous signals stimulated researchers to develop new DSP algorithms, such as evaluation and simulation. First of all, it should be noted that the Kotel'nikov theorem only solves the problem of interpolating a function in the course of sampling it in an infinite time interval, $-\infty < t < +\infty$. In practice, one always deals with a *finite observation time interval*, and it is necessary to not only interpolate a function on a finite interval but also perform filtration, i.e., evaluate the function at some instants of time from its samplings in the interval from 0 to t, as well as extrapolation, i.e., predicting the function values at instants of time $T > t$ from its samplings in the interval from 0 to t. Therefore, it was important to develop algorithms for restoring the values of a function within the intervals between discrete samplings, i.e., at the instants t of time falling between the values of t_i and t_{i+1}. In other words, the infinite series (1) was to be substituted by a finite series. For practical implementations, extrapolators of various complexity were developed, most of them in the form of power series, Lagrange polynomials, splines, atomic functions, etc. [2].

Results obtained by Kotel'nikov stimulated a series of works aimed at eliminating the following restrictions adopted in the proof of Kotel'nikov's theorem [3–7]:

(1) fixed zero initial sampling;

(2) infinite spectrum of real stochastic signals;

(3) complexity of calculations for restoring the function by means of series (1) and (2);

(4) nonuniformity of the samplings;

(5) bunching of the samplings;

(6) impossibility to find the statistical characteristics of errors during the sampling;

(7) impossibility to take into account the errors of measuring the function at sampling points t_i;

(8) impossibility to take into account the errors caused by a limited digitization capacity for the series (1) and (2), etc.

5. Filtration and simulation of continuous processes from discrete observations and Kotel'nikov's theorem

It is well known [8] that principally new prospects for creating algorithms for filtering a continuous signal from discrete measurements opened up after the works by R Kalman, where the desired signal was represented as a solution to a linear stochastic differential equation. Let us consider a system whose state at any instant of time is unambiguously determined by a certain set of phase variables (output coordinates and their derivatives), which are not measurable directly. In addition, there are some variables related somehow to the state of the system, which can be measured at some discrete instants of time with a given accuracy. Kalman considered coordinate filtration in the conditions where the desired signal was described by continuous stochastic differential equations and the measurements were continuous, as well as in cases where the desired signal was described by a recurrent random sequence (the discrete-variable analogue of a stochastic differential equation) and measurements occurred at discrete instants of time. In Ref. [9], the problem of controlling such measurements was formulated and solved.

Computer realizations of a Kalman filter rely on the following two important facts.

(1) The matrix amplification coefficient of a filter is found by solving the discrete nonlinear Riccati equation. The conditional covariance matrix for the filtration errors is 'desymmetrized' due to the finite capacity of digital computers (DCs).

(2) In a computer simulation of a real process, models with continuous sets of states are substituted by models with discrete sets of states, which causes additional distortions of the results. The reason of such a complication is that any discretization procedure represents a fundamentally nonlinear (moreover, discontinuous) mapping, which introduces considerable distortions into the processed signal. *The effect of such distortions can also be qualitatively explained in terms*

of Kotel'nikov's theorem; however, a quantitative description of this effect is connected with considerable technical difficulties and fundamental theoretical problems. It should be noted that, unfortunately, this phenomenon is not sufficiently considered in the literature; therefore, let us dwell on it a bit more.

6. Two fundamental questions in computer simulations

First. The final goal of computer simulation is obtaining *information* about the object under study. But then, one should take into account that while it is often possible to pass from one continuous model to another without the loss of information (homeomorphous changes of variables, etc.), *passing from a continuous object to a discrete model, as a rule, leads to information loss*. A simple example is discretization of a reversible linear system on a uniform lattice: as a rule, it is an irreversible mapping. Another example considers the main information characteristic of a dynamical system, its entropy. The entropy is a measure of the exponential increase in the ratio of the number of different trajectories of the system to their length. However, any unambiguous spatial discretization of a system allows only a limited number of infinite trajectories, and the definition of entropy becomes meaningless in this case. Here, we have an evident contradiction between a continuous object and its discrete model; also evident is the necessity to improve the methods of evaluating the entropy of a continuous system from its discretizations. Notice that although different methods of solving this problem have already been proposed, the general task is very difficult to solve. In other cases, the conflict may be less evident but not less dangerous. Hence, the first fundamental question of every computer simulation is: *What is the information loss for the chosen scheme of passing from a continuous object to a discrete one*?

Second. The question is related to the continuous-mathematics analogues of robustness and structural stability. In continuous simulations, if one omits verbal descriptions, this is the question of whether one property or another of the object is tolerant to continuous, smooth, etc. (but necessarily small in some continuous sense) perturbations. However, if we accept that the main point of computer simulations is related to information, we should also pose the following question: *Can we guarantee the information robustness of the chosen scheme of passage from the continuous object to the discrete one*?

Probably, thorough analysis of these questions will be one of the strategic areas of natural sciences in the nearest decades. To give an overall description of the situation in this field is a hopeless task, even more so to predict its development. Some initial progress in this area is reported in Refs [10–12].

This work was supported in part by RFBR (projects Nos 06-01-00256 and 07-07-00031).

References

1. Kotel'nikov V A "O propusknoi sposobnosti 'efira' i provoloki v elektrosvyazi" ("On the transmission capacity of 'ether' and wire in electric communications"), in *Vsesoyuznyi Energeticheskii Komitet. Materialy k I Vsesoyuznomu S'ezdu po Voprosam Tekhnicheskoi Rekonstruktsii Dela Svyazi i Razvitiya Slabotochnoi Promyshlennosti* (The All-Union Energy Committee. Materials for the 1st All-Union Congress on the Technical Reconstruction of Communication Facilities and Progress in the Low-Currents Industry) (Moscow: Upravlenie Svyazi RKKA, 1933) p. 1; second edition: *O Propusknoi Sposobnosti 'Efira' i Provoloki v Elektrosvyazi* (On the Transmission Capacity of 'Ether' and Wire in Electric Communications) (Moscow: Inst. Radiotekhniki i Elektroniki MEI (TU), 2003); *Usp. Fiz. Nauk* **176** 762 (2006) [*Phys. Usp.* **49** 736 (2006)]
2. Kravchenko V F, Rvachev V L *Algebra Logiki, Atomarnye Funktsii i Veivlety v Fizicheskikh Prilozheniyakh* (Algebra of Logics, Atomic Functions and Wavelets in Physical Applications) (Moscow: Fizmatlit, 2006)
3. Whittaker E T "On the functions which are represented by the expansion of interpolating theory" *Proc. R. Edinburgh* (35) 181 (1915)
4. Balakrishnan A V "A note of the sampling principle for continuous signals" *IEEE Trans. Inform. Theory* **3** 143 (1957)
5. Belyaev Yu K "Analiticheskie sluchainye protsessy" ("Analytical random processes") *Teoriya Veroyatnostei Ee Primeneniya* (4) 402 (1959)
6. Beutler F J "Sampling theorems and basis in a Hilbert space" *Inform. Control* (4) 97 (1961)
7. Jerri A J "The Shannon sampling theorem — its various extensions and applications: a tutorial review" *Proc. IEEE* (65) 1565 (1977)
8. Sinitsyn I N *Fil'try Kalmana i Pugacheva* (Kalman and Pugachev Filters) (Moscow: Logos, 1st ed. — 2005, 2nd ed. — 2007)
9. Grigor'ev F N, Kuznetsov N A, Serebrovskii A P *Upravlenie Nablyudeniyami v Avtomaticheskikh Sistemakh* (Control of Observations in Automatic Systems) (Moscow: Nauka, 1986)
10. Kozyakin V S, Kuznetsov N A "Dostovernost' komp'yuternogo modelirovaniya s tochki zreniya teorii informatsii" ("Reliability of computer simulations from the standpoint of information theory") *Informatsionnye Protsessy* **7** 323 (2007); http://www.jip.ru/2007/323-368-2007.pdf
11. Vladimirov I "Quantized linear systems on integer lattices: Frequency-based approach. Part I", CADSEM Report 96-032 (Geelong, Australia: Deakin Univ., 1996)
12. Diamond P, Vladimirov I "Higher-order terms in asymptotic expansion for information loss in quantized random processes" *Circuits, Systems, Signal Process.* **20** 677 (2001)

PACS numbers: **43.30.+m**, **43.58.+z**, 91.50.Ga
DOI: 10.3367/UFNe.0179.200902k.0218

Remote sensing of sea bottom by hydroacoustic systems with complex signals

V I Kaevitser, V M Razmanov

1. Introduction

This report deals with various aspects of applying complex sounding signals with linear frequency modulation (LFM) in hydroacoustic systems (including a multielement antenna) for the exploration of the ocean floor. The report presents a review of theoretical and practical results obtained by authors recently in the course of the development, testing, and implementation under different conditions of the following hydroacoustic systems: acoustic low-frequency linear profilographs, surveillance and interferometric side-looking sonars (SLSs), and multibeam echo sounders.

The radar exploration of planets that was conducted starting in the late 1950s by the group of scientists under the leadership of V A Kotel'nikov resulted in establishing at the Institute of Radioengineering and Electronics (IRE) of the USSR Academy of Sciences (now the Russian Academy of Sciences — RAS) a new field of research — remote mapping of extended objects by high-energy complex sounding signals and digital methods of coherent processing of echo signals. The digital methods of signal synthesizing, recording, and processing, used earlier for planetary radar, in late 1970s were

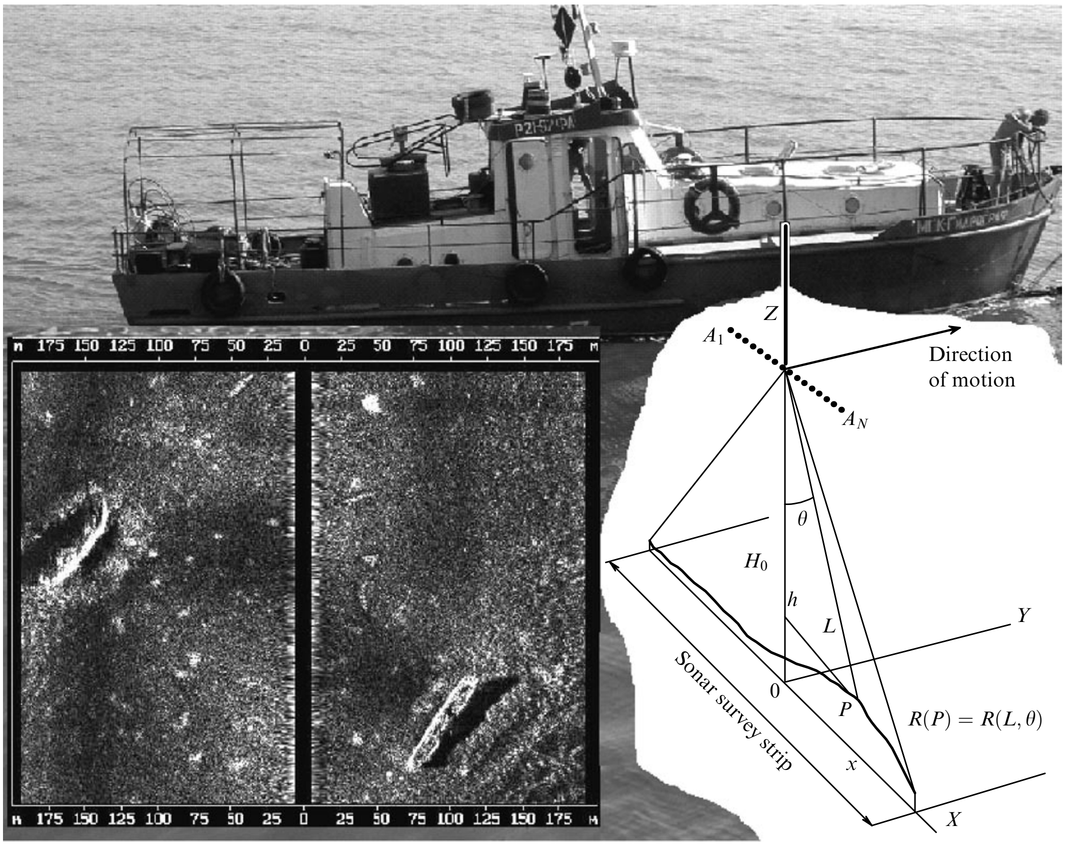

Figure 1. Geometrical sketch of a side-looking sonar survey and a detail of an obtained seafloor acoustic image depicting sunken vessels.

successfully applied to develop a new generation of hydroacoustic systems for seafloor mapping.

Nowadays, the hydroacoustic systems of coherent radar sounding have become the primary tool for remote measurements of the undersea relief and structure of sea bottom deposits. By now, two main classes of systems (somewhat competing with each other) aimed at synchronous measurements of seafloor relief and acquiring bottom surface acoustic images have been developed: interferometric SLSs and multibeam echo sounders [1]. While the surveillance SLS usually contains one onboard antenna and interferometric SLSs two or three antennas, multibeam echo sounders constitute a more complicated system that contains a significantly higher number of receiving elements, usually 100 or more. The studies of subsurface structure of a sea bottom employ low-frequency acoustic profilographs. These are usually one-channel systems that provide continuous profiling of a seabed along a vessel route. The exploration systems are equipped with satellite navigation GPS (Global Positioning System)/DGPS (Differential Global Positioning System), devices for measuring the speed of sound in deep water, and sensors to monitor roll, pitch, and vertical displacements of the vessel. In complex multielement systems, usage of stabilizing equipment reducing vessel rolling effects is justified.

The operational efficiency of coherent sonar systems is determined by the type of sounding signals. For shallow water exploration (up to 100 m in depth), SLS and multibeam echo sounder systems use short sounding pulses with a carrier frequency of up to 500 kHz due to the simplicity of their formation and treatment. For deep water exploration, contemporary systems utilize sounding signals with linear modulation frequency that combine both high-energy capacity and high time resolution.

2. Diagram of side-looking survey

Hydroacoustic methods of side-looking surveys are based on sequential accumulation of seafloor data while the vessel is moving (Fig. 1). The acoustic pulse radiated by the transmitting antenna is sequentially reflected from seafloor elements at different distances. The reflected echo signals are acquired by one or more receiving antennas. The cycle that consists of a pulse transmission and a signal reception forms one realization (one horizontal row of the acoustic image in Fig. 1). A set of sequential realizations that is formed during the vessel movement contains information about scattering characteristics of a seafloor within the sonar survey strip and represents the acoustic image of the floor, similar to optical and radar images. These acoustic images are aimed at visualization and classification of objects. For example, the inset to Fig. 1 shows a detail of the acoustic image of a seafloor area that reveals the fragments of two sunken vessels. The sonar survey strip which is determined by the antenna patterns of receiving elements, power characteristics and the shape of undersea relief is usually set in units of depth H_0, equaling $(4-10)H_0$. The use of antennas with narrow side-looking patterns provides a distinct type of 2-dimensional measurement in a plane of side-looking survey. The seafloor is perceived as a medium with the back scattering factor $R = R(L, \theta)$ dependent on distance L and angle θ between the vertical line and the direction of a signal arriving in a plane of side-looking survey. Considering a coefficient of reflection $R = R(u, \tau)$ as a function of two parameters, namely, the angle parameter $u = \sin\theta$ and time delay τ, the signal $Z_n(t)$ received by a particular antenna in multielement antenna system can be expressed as

$$Z_n(t) = \iint R(u,\tau)\, S_0(t-\tau-\tau_n u)\, \mathrm{d}u\, \mathrm{d}\tau\,, \quad u = \sin\theta\,. \quad (1)$$

Distance L is related to the propagation time (delay) τ as $\tau = 2L/c$, where c is the speed of sound. Additional delay $\tau_n = l_n/c$ caused by geometrical differences in paths at which echo signals reach the various elements of the antenna is determined by coordinate l_n of a particular element in the antenna coordinate system.

In many practical instances that employ complex signals, model (1) can be simplified, limiting itself to a narrow-band approximation. With this in mind, we can present $S_0(t)$ as $S_0(t) = \exp(\mathrm{i}\omega_0 t)\, S_{\mathrm{A}}(t)$, where ω_0 is a carrier frequency, and $S_{\mathrm{A}}(t)$ is a slowly varying component of modulation. Signal $S_0(t)$ will be considered as a narrow-band signal, assuming that under $\Delta t \ll t_0$ the expression $S_{\mathrm{A}}(t+\Delta t) \approx S_{\mathrm{A}}(t)$ is true. As a result, for $\Delta t \ll t_0$ we arrive at the following relationship for a narrow-band signal: $S_0(t_0+\Delta t) \approx \exp(\mathrm{i}\omega_0\Delta t)\, S_0(t_0)$. Considering arrival time delay $\tau_n u$ on individual elements of the array as small parameter Δt of theory, in other words, given that $\tau_n u \ll t-\tau$ is true, measurement model (1) can be presented as follows:

$$\begin{aligned} Z_n(t) &= \iint R(u,\tau)\, S_0(t-\tau) \exp(-\mathrm{i}\omega_0\tau_n u)\, \mathrm{d}u\, \mathrm{d}\tau \\ &= \int R_t(u) \exp\left(-2\pi\mathrm{i}\, \frac{l_n}{\lambda}\, u\right) \mathrm{d}u\,, \end{aligned} \quad (2)$$

where $R_t(u) = \int R(u,\tau)\, S_0(t-\tau)\, \mathrm{d}\tau$, and λ is a wavelength that is related to the carrier frequency ω_0. For fixed distances, the determination of the reflection coefficient is a task of spectral estimation, i.e., assessment of the acoustical spectrum of a signal based on a set of its discrete samples Z_n:

$$Z_n = \int R_t(u) \exp\left(-2\pi\mathrm{i}\, \frac{l_n}{\lambda}\, u\right) \mathrm{d}u\,. \quad (2a)$$

Here, $R_t(u)$ can be considered the angular spectrum that may be estimated by the well-known spectral analysis methods of both a parametric and nonparametric nature [2, 3]. The task of data processing is the estimation of reflection coefficient $R(u,\tau)$ based on a set of measurements of $Z_n(t)$ and subsequent determination of parameters of a seafloor. The applied methods of estimation of the reflection coefficient R and parameters of a seafloor, as well as various limitations related to variations in the shape of an undersea relief, differ from each other depending on the number of receiving antennas in the measuring systems employed.

3. One-channel systems with linear-frequency-modulated signals: acoustic profilographs and surveillance side-looking sonars

In one-channel systems, in the absence of angular selectivity, measurement model (1) degenerates into the relationship for the coefficient $R = R(\tau)$ which is dependent on delay τ (distance L) only; thus, the registered signal is described as

$$Z(t) = \int R(\tau)\, S_0(t-\tau)\, \mathrm{d}\tau\,.$$

In a mean-square metric, the $R(\tau)$ estimate should minimize the functional

$$\begin{aligned} \varDelta = \int \mathrm{d}t \left(Z - \int S_0(\tau)\, R(t-\tau)\, \mathrm{d}\tau\right) \\ \times \left(Z^* - \int S_0^*(\tau)\, R^*(t-\tau)\, \mathrm{d}\tau\right). \end{aligned} \quad (3)$$

The optimum estimate of $R(t)$ must satisfy the Fredholm integral first-order equation

$$\int Z(t+\tau)\, S_0^*(\tau)\, \mathrm{d}\tau = \int R(t-\tau)\, K_0(\tau)\, \mathrm{d}\tau\,, \quad (4)$$

where the kernel is determined by the correlation function of a sounding signal:

$$K_0(\tau) = \int S_0(t)\, S_0^*(t+\tau)\, \mathrm{d}t\,.$$

For LFM signal $S_0(t) = \exp\left(\mathrm{i}\omega_0 t + \mathrm{i}(\Delta\omega/2T)t^2\right)$, the correlation function looks like

$$K_0(\tau) = \exp\left(\mathrm{i}\varPhi(\tau)\right) \frac{\sin\left[\pi B(\tau/T_0)\left(1-|\tau|/T_0\right)\right]}{\pi B\tau/T_0}\,, \quad (5)$$

where $\varPhi(\tau) = -(\omega_0 + \pi B/T)\tau$, B is a base of a signal, defined as $T_0\Delta\omega = 2\pi B$, T_0 is a pulse length, and $\Delta\omega$ is a bandwidth.

Strictly speaking, equation (4) falls into a class of ill-posed problems. A number of methods that allow solving these problems use various additional assumptions about the changing character of $R(\tau)$ [4]. In practice, relationship (4) is employed as a ready-made algorithm of approximate estimation of $\tilde{R}(\tau)$ for a given resolution. To demonstrate it we present expression (4) as two relationships:

$$\tilde{R}(t) = \int Z(t+\tau)\, S_0^*(\tau)\, \mathrm{d}\tau\,, \quad (6a)$$

$$\tilde{R}(t) = \int R(t-\tau)\, K_0(\tau)\, \mathrm{d}\tau\,. \quad (6b)$$

Relationship (6a) can be regarded as a treatment algorithm that is realized in a spectral range with the help of fast Fourier transform (FFT) algorithms. The operation of a signal compression is the price for employing complex signals. Relationship (6b) defines resolution of the $\tilde{R}(\tau)$ estimate as a convolution of the exact solution with the kernel $K_0(\tau)$ — the correlation function of a sounding signal. For tone signals, the correlation interval (area where the value of $|K_0(\tau)|$ differs from zero significantly) is determined by the pulse duration T_0. The main advantage of employing LFM-probing signals is that due to intrapulse modulation the correlation interval decreases to T_i/B, where B is a signal base. This allows us to combine high energy potential with high (up to fractions of the centimeter) resolution.

The dependence of the modulus of reflection coefficient R on the distance serves as the basis for acoustic seafloor mapping. The absence of angular selectivity in one-channel surveillance SLSs does not prevent employing this class of systems for exploration of relatively flat seafloor areas in searching for small-sized objects and details of undersea relief such as furrows, trenches, and stones. Usually, the surveillance SLS constitutes a one-channel acoustic sonar mounted on the right and left sides of the shipboard and is equipped

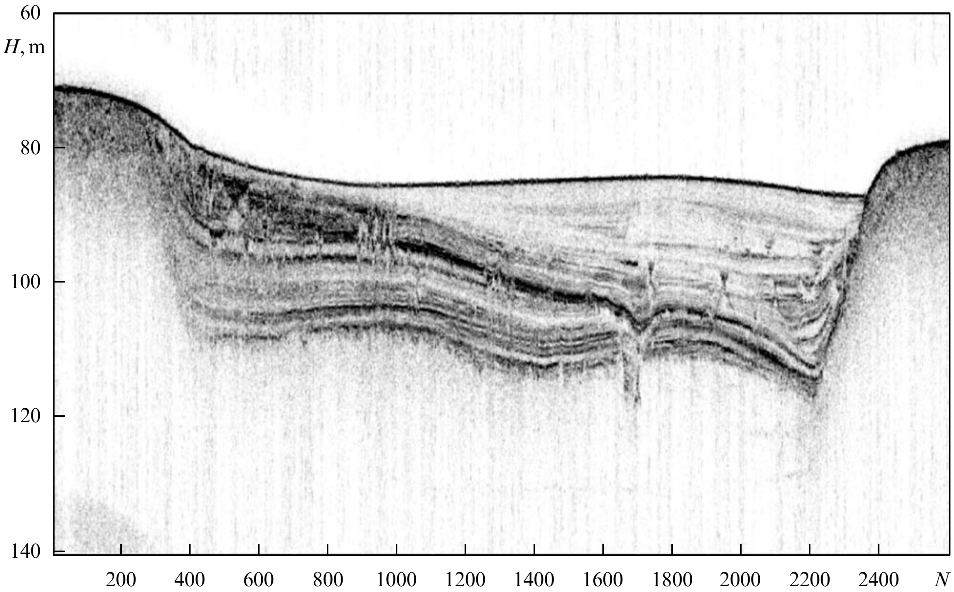

Figure 2. Profile of undersea relief and sedimentary rocks (Chukchi Sea). Probable ancient riverbed.

with independent transceiver antennas having a narrow (around 1°) directional pattern along the route of a vessel, as well as a digital system for generating, recording, and treating signals. The type of radiated pulse comprises both tonal and LFM sendings. Operating frequencies fall within 10–500 kHz. In tonal mode, the pulse duration is several fractions of a millisecond, while in LFM mode it reaches several seconds.

Among one-channel devices that broadly employ LFM signals in experimental samples are acoustic linear profilographs. Many years of experience using low-frequency profilographs with LFM-probing signals (the ones that have been developed at IRE RAS) has confirmed their good operational abilities and helped to reveal some specifics in interpreting obtained results. The profilograph operating frequency equals 5 kHz, band frequency is around 4 kHz, and radiated power is near 3 kW. The profilograph comprises a 9-element antenna system, electronic system for generating probing sonar signals (digital synthesizer), sound projector, and computer data input interface. The device contains a digital system for collecting, mapping, and processing data. It is intended for use in exploration of a seafloor topography and structure of sea bottom deposits in a range of depths from 20 to 3000 m. Data collection programs provide coherent engagement of echo signals, input of navigational information about vessel location from GPS sensors, real-time data imaging, and archiving of the processed data.

Figure 2 shows a detail of an undersea relief that was acquired in the course of seabed profiling in the deep freezing waters of the Chukchi Sea at a depth of approximately 70 m. The result of profiling shows high interference immunity of the device, providing a high-resolution image of seabed deposits. The above detail attracts more interest because it clearly depicts a depression filled with deposits. This image resembles a riverbed of an ancient river after the land submerged as a result of a rise in the sea level. The offered hypothesis may serve as a very productive approach to solving some problems in the course of establishing continental shelf boarders.

The high energy potential of LFM-probing signals allows conducting the profiling of seabed deposits at quite large depths. Figure 3 presents the results of profiling in the Sea of Japan at depths of 1200–1400 m. The studied area is characterized by varying relief with a thick stratum of layered deposits. The first reflection corresponds to the depth and it is confirmed by the measurements made with single- and multibeam echo sounders. The horizontal axis is the distance travelled in meters; the vertical axis is the depth in meters. As indicated in Fig. 3, the depth of profiling is more than 100 m; slope deposits have the layered structure which is typical of silted clay. In the area of the depression, the character of the profilogram is more homogeneous over the depth, typical of sandy clay soils.

4. Signals with linear frequency modulation in interferometric side-looking sonars

The complex interferometric SLS system that is used for the analysis of an undersea relief within the sonar survey strip includes additional receiving channels that contain a set of antennas in a vertical plane. In interferometric SLSs, signal processing is based on the assumption that at any given distance the present signal propagates in a single direction: $R(u,\tau) = R(\tau)\,\delta\big[u - u_0(\tau)\big]$, therefore, reception model (2) in a narrow-strip approximation becomes

$$Z_n(t) = R(t)\exp\left[2\pi\mathrm{i}\,\frac{l_n}{\lambda}\,u_0(\tau)\right],$$

where $R(t) = \int R(\tau)\,S_0(t-\tau)\,\mathrm{d}\tau$, and $u_0 = \sin\theta_0$. The determination of reflection coefficient $R(t)$ is exactly the same as in a surveillance SLS. To calculate the angle of signal arrival we need to measure the phase Ψ of a complex-conjugate product of the pair of samples in two channels (interferometer):

$$A_{n,m}(t) = Z_n(t)Z_m^*(t) = \big|R(t)\big|^2\exp\Psi_{n,m}\,, \qquad (7)$$

$$\Psi_{n,m} = \arctan\frac{\operatorname{Im}A_{n,m}}{\operatorname{Re}A_{n,m}}\,.$$

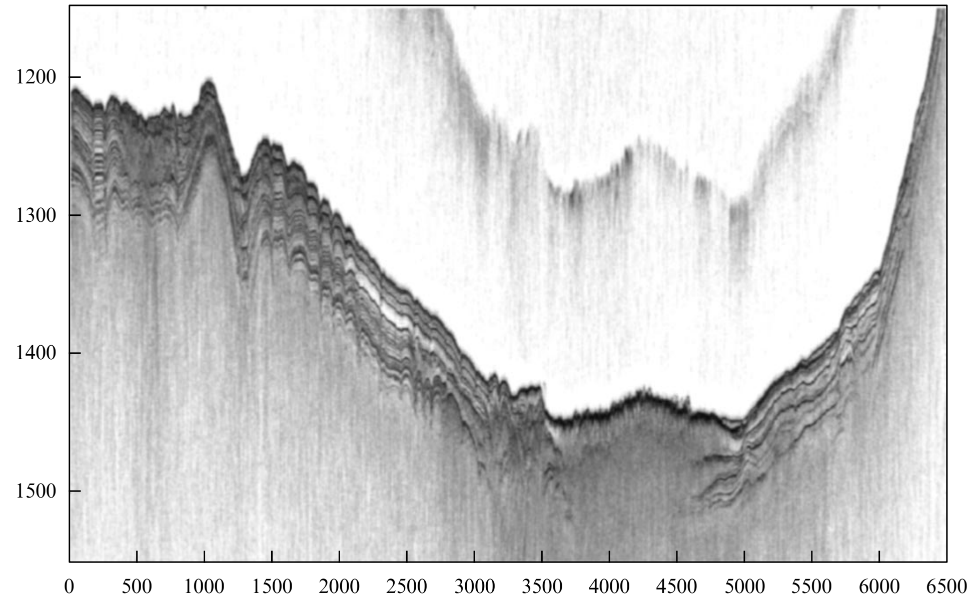

Figure 3. Detail of profiling a sea bottom deposit in the Sea of Japan at depths of up to 1500 m. The depth of profiling the subsurface bottom structures is more than 100 m.

The interference phase is related to both the angle of arrival θ and the interferometer base $b_{nm} = l_n - l_m$ as follows:

$$\Psi_{n,m}(t) = \exp\left[2\pi\mathrm{i}\,\frac{b_{nm}}{\lambda}\,\sin\theta(t)\right].$$

The phase is used to calculate the angle of arrival, while the depth h and horizontal coordinate x of the reflection element (relief) are calculated from the distance L and angle of arrival θ using the relationships

$$h = L\cos\theta\,, \qquad x = L\sin\theta\,. \tag{8}$$

The details of processing the data obtained by interferometric SLSs are described in Refs [6, 7].

Commonly used interferometric SLSs contain 2–3 antennas on each side of a shipboard (several interferometers), a satellite navigation system, devices for profiling the speed of sound, and sensors to monitor the roll, pitch, and vertical displacements of a vessel. Similar to one-channel systems, interferometric SLSs have a directional pattern that is narrow (near 1°) along the line of motion and rather wide (near 60°) in the plane of the side-looking sonar survey. This type of acoustic system is broadly used since it is easy to operate and has a wide survey strip of observation. These systems produce high-quality acoustic images and at the same time allow measuring the depths within the survey strip.

Various modifications of experimental interferometric SLSs developed at IRE RAS have been successfully employed in different applications from river floor soundings to a large-scale exploratory projects carried out on large-capacity ships in the deep freezing waters of the Arctic Ocean [5–7]. Surveying work in shallow waters (up to 100 m) mostly employs tone acoustic pulses that do not require any compression. On the other hand, work in deep waters employs LFM signals of various duration depending on depth and the desired energy characteristics.

We have to note the important differences in applying tone and LFM signals. In acoustic images created by tone signals, the prime elements on both the left and right sides contain a characteristic flare. This is caused by amplitude overload of the detectors. In practice, it significantly complicates the circuitry of the receiving device because it requires engaging a temporal automatic gain control (TAGC) for each reception row. This imposes considerable difficulties in data processing and requires manual operator intervention. The quality of produced images greatly depends on acoustic noises of various natures. In coherent processing of complex signals, the extraction of useful information is done along the frequency rather than amplitude characteristics. This problem is nonexistent when coherence of echo signals is retained. In such cases, the use of a conventional system of AGC is a sufficient means for matching a level of output signal with the dynamic range of the analog-to-digital converter (ADC). The latter provides an important advantage to the above remote sounding systems in uncrewed submersible vehicles and in cases of significant amplitude interferences.

Figure 4 depicts details of acoustic images obtained in the course of studying the route of an undersea optical cable in the icy conditions of the Arctic Ocean. Figure 4a shows traces of sea bottom exaration caused by a large iceberg, and Fig. 4b demonstrates trenches of the same nature. The complex trajectory of the trenches is related to the changing direction of underwater currents. Besides images of the objects themselves, the acoustic images contain information about the acoustic density of a sea bottom surface. The difference in back scattering factors is determined by the degree of background brightness. It carries information about the geological bedrock on the sea bottom. Figure 5 presents a detail of a bathymetric chart built on the results of interferometric measurements. Halftone images exhibit the fluctuations in seabed density.

The main deficiency of interferometric systems is the distortions in the selectivity of signals detected with the same delay with respect to the angle of arrival. This results in limitations on using these systems in multibeam applications, as well as in cases of a complex undersea relief, etc. [6]. Multielement systems are free of such limitations; they allow separating signals coming from different directions (para-

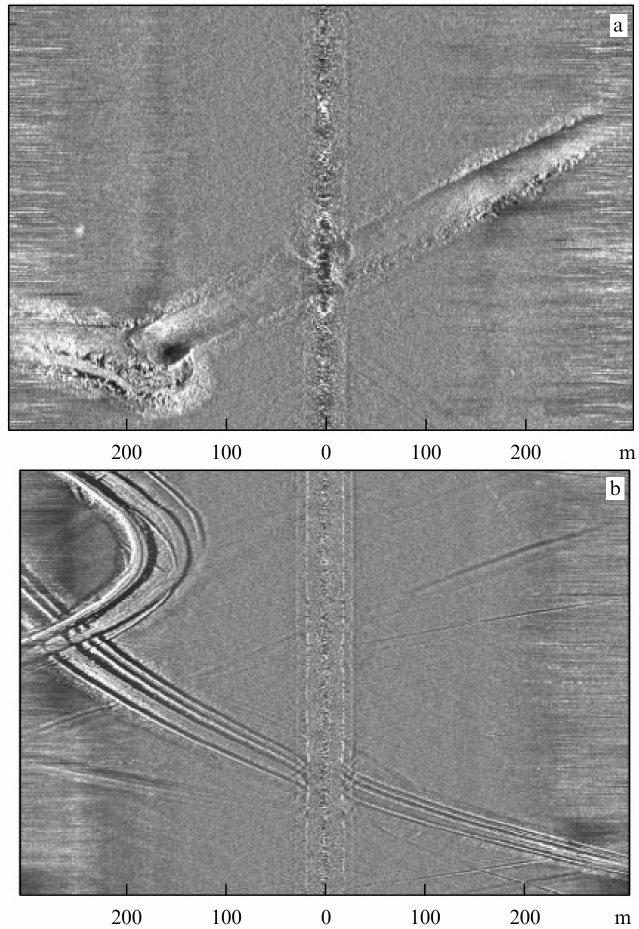

Figure 4. Details of acoustic images provided by an interferometric SLS with an LFM-probing signal: (a) bottom tracks are traces of exaration caused by a large iceberg in the Arctic Sea at a depth of 20 – 30 m; the vertical length of the detail is 1 km; (b) ice exaration that characterizes the trajectory of iceberg movement in changing currents; vertical length of the detail is around 2 km.

metric approach) or signals with high angular resolution (nonparametric methods).

5. Miltibeam echo sounder with linear-frequency-modulated sounding signals

In a multielement array and in measurement model (1), the mean-square criterion (3) for estimation of the reflection coefficient takes the form

$$\Delta = \sum_n \int \left| Z_n(t) - \int R(u,\tau)\, S_0(t-\tau-\tau_n u)\, \mathrm{d}u\, \mathrm{d}\tau \right|^2 \mathrm{d}t\,,$$

while the equation for the estimate is written out as

$$\sum_n \int Z_n(t)\, S_0^*(t-\tau_0-\tau_n u_0)\, \mathrm{d}t = \int R(u,\tau) \left\{ \sum_n K_0\big(\tau-\tau_0-\tau_n(u-u_0)\big) \right\} \mathrm{d}u\, \mathrm{d}\tau\,.$$

The kernel (enclosed in curly brackets) of the integral equation describes the resolution in angle and distance. In the narrow-band approximation, the kernel degenerates into a product of two factors dependent on angle and distance:

$$\sum_n \tilde{Z}_n(t) \exp\left(2\pi \mathrm{i}\, \frac{l_n}{\lambda}\, u_0\right) = \int R(u,\tau)\, K_0(\tau-t)\, K_\theta(u-u_0)\, \mathrm{d}u\, \mathrm{d}\tau\,, \qquad (9)$$

where $\tilde{Z}_n(t) = \int Z_n(t)\, S_0^*(t-\tau_0)\, \mathrm{d}t$ is the compressed input data, and $K_\theta(u-u_0) = \sum_n \exp\big(-2\pi \mathrm{i} (l_n/\lambda)(u-u_0)\big)$ is a directional pattern of the array. Similar to the equation from Section 3, equation (9) can be considered an estimate of the reflection coefficient $\tilde{R}(u,\tau)$ within the framework of time resolution of the correlation function $K_0(\tau)$ and angular resolution of directional pattern $K_\theta(u)$:

$$\tilde{R}(u,t) = \sum_n \tilde{Z}_n(t) \exp\left(2\pi \mathrm{i}\, \frac{l_n}{\lambda}\, u_0\right). \qquad (10)$$

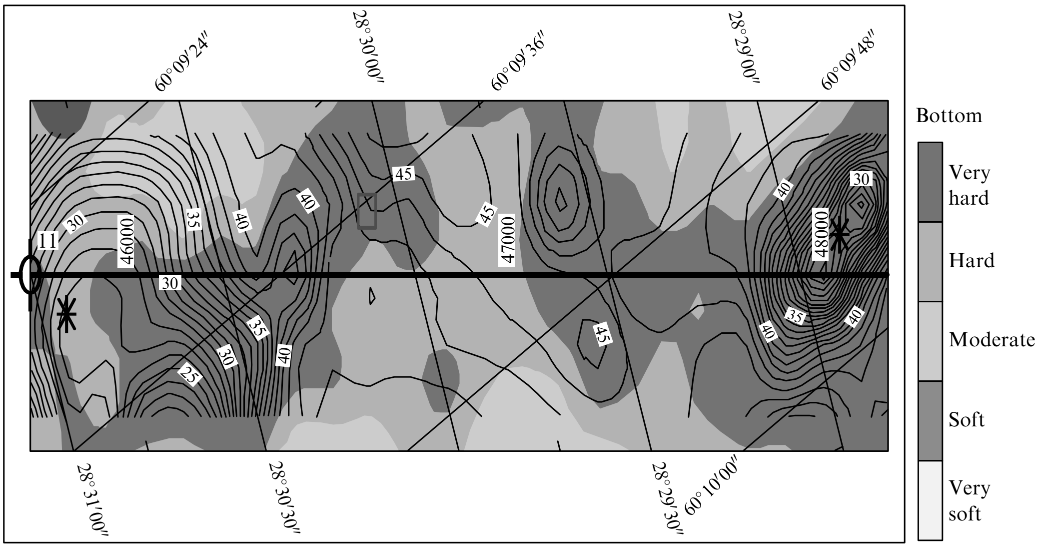

Scale 1:10000, Ellipsoid WGS84, Projection UTM, Center Meridian27°

Figure 5. Portion of a bathymetric chart in the form of contour lines of depths (isobaths). The isobaths shown have a 5-m pitch. The halftone background marks the acoustic density of the bottom.

In this case, signal processing constitutes a compression of input samples in all channels and Fourier transformation of these samples for each distance. For a fixed pattern, especially with a small number of receiving antennas, an increase in spatial resolution becomes an important practical goal. The solution to this problem can be found with the help of both equation (9) (nonparametrical approach) and the use of parametrical algorithms of spectral estimation [2–4].

The first tests of an experimental system with a multi-element antenna and LFM-probing signals were conducted at IRE RAS in 2007 at an aquatorium on the Sea of Japan. This hydroacoustic system consists of a linear transmitting and 32-element receiving antenna system (modelled on the Mills cross), powerful amplifier of radiated signals, digital generator (synthesizer) of LFM signals, and 32-channel low-noise digital receiver with computer input data interface. The carrier frequency of sounding signals is 30 kHz, frequency deviation is 3.0 kHz. Signal quantization was carried out at a frequency of ~ 6.0 kHz in each of the channels. The distance between receiving elements of the antenna array is a half wavelength of the radiated signal at the carrier frequency.

In accordance with formula (10), compression in all 32 channels of signals was carried out initially. The calculation of the angular spectrum for each distance was performed with the help of FFT with $N = 32$ dimensions (in some cases a larger dimension, up to $N = 256$, was used) and by weighting the input channel samples for different variants of weighted sequences. In this case, the set of spectral samples forms a system of partial beams. The angular position $u_m = \sin\theta_m$ of a beam with number (spectral sample) m for distance d between receiving elements of an antenna with a half wavelength λ is derived from relationship $u_m = \lambda m/(dN) = 2m/N$, where $m = 0, \ldots, N-1$, N is the FFT dimension, and the angle θ is measured from the antenna normal. Beam amplitude reaches its maximum at a distance corresponding to the point where the beam crosses the sea bottom. The generation of the undersea relief was performed using slant range L, which had been determined by the position of the amplitude maximum peak in each beam with a known angle of inclination in accordance with expressions (8). Examples of variation of beam amplitude near the maximum are shown in Fig. 6 and characterize two extreme types of data. For the first group of data (in the left part of Fig. 6a), the peak near the maximum is wide, and its amplitude smoothly decreases along the ascending beam number (angle of inclination), shifting in distance. The FFT algorithm applied to the spatial diagram forms a good image of a seafloor relief (an example of this type of relief is shown in Fig. 6b). For a second group of data (in the right part of Fig. 6a), the shape of the amplitude near the maximum looks like a narrow peak along almost the same distance; the peak amplitude declines sharply with ascending beam number. The treatment of data revealed that the use of FFT in such cases is inefficient due to a high level of side lobes; therefore, estimation of the angular spectrum was performed on the basis of the autoregressive parametric method (Proni method) [2]. This demonstrates good timing for the development and application of spectral methods of estimation with high resolution in multibeam systems.

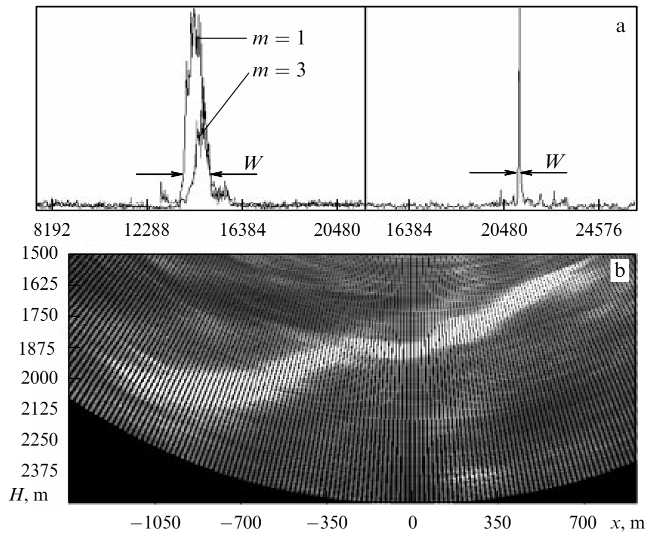

Figure 6. Variation of echo signal amplitude of individual beams versus distance (sample number); m is the beam number. The sampling period corresponds to a distance interval of 0.1 m. (Obtained in the course of probing various types of bottom soils.) (b) Example of relief extraction from the system of spatial beams.

6. Conclusion

The presented results of theoretical analysis and developed algorithms of signal processing in various hydroacoustic systems with LFM-probing signals for remote seafloor exploration have been implemented and tested under different conditions, including complicated operation in Arctic waters.

This report outlines only some aspects of treating data in LFM-signal applications. Certain important issues, such as methods of secondary data treatment, the construction of bathymetrical maps and maps of brightness, preparation of various reports, and documenting the results, are beyond the scope of this presentation.

The conducted experiments have proved the important advantages of such development projects in comparison with traditional hydroacoustic sonars that employ tone sounding pulses. These advantages include an increase in energy potential and resolution; higher interference immunity that results in improved electrical and acoustical compatibility of various devices, and increased potential for automation of various hydroacoustic systems.

Besides the above aspects, the application of coherent methods of LFM-signal processing in promising projects will in the future allow employing additional signal characteristics that may become important classification criteria for interpreting the results of remote sea bottom studies [8].

References

1. Costnel C, Yoos L T *Sea Technol.* (March) (2007)
2. Marple S L *Digital Spectral Analysis: with Applications* (Englewood Cliffs, NJ: Prentice-Hall, 1987) [Translated into Russian (Moscow: Mir, 1990)]
3. Leonowicz Z, Lobos T, Rezmer J *IEEE Trans. Industrial Electron.* **50** 514 (2003)
4. Vasilenko G I *Teoriya Vosstanovleniya Signalov* (Theory of Signal Reconstruction) (Moscow: Sov. Radio, 1979)
5. Kaevitser V I et al. *Radiotekhnika* (1) 42 (2004)
6. Kaevitser V I, Razmanov V M *Radiotekhnika* (12) (2005)
7. Razmanov V M, Krivtsov A P, Dolotov S A *Radiotekh. Elektron.* **51** 58 (2006) [*J. Commun. Technol. Electron.* **51** 52 (2006)]
8. Gulyaev Yu V, Zakharov A I, Kaevitser V I *Dokl. Ross. Akad. Nauk* **413** 257 (2007) [*Dokl. Earth Sci.* **413** 327 (2007)]